© Springer-Verlag 2004

ORIGINAL PAPER

W. C. Tennant · R. F. C. Claridge · C. J. Walsby · N. S. Lees

Point defects in crystalline zircon (zirconium silicate), ZrSiO₄: electron paramagnetic resonance studies

Abstract This article outlines the present state of knowledge of paramagnetic defects in crystalline zircon as obtained mainly, but not exclusively, from electron paramagnetic resonance (EPR) studies in crystalline zircon (zirconium silicate, $ZrSiO_4$). The emphasis is on single-crystal studies where, in principle, unambiguous analysis is possible. Firstly, the crystallography of zircon is presented. Secondly, the relationships between available crystal-site symmetries and the symmetries of observed paramagnetic species in zircon, and how these observations lead to unambiguous assignments of point-group symmetries for particular paramagnetic species are detailed. Next, spin-Hamiltonian (SH) analysis is discussed with emphasis on the symmetry relationships that necessarily exist amongst the Laue classes of the crystal sites in zircon, the paramagnetic species occupying those sites and the SH itself. The final sections of the article then survey the results of EPR studies on zircon over the period 1960–2002.

Keywords Electron paramagnetic resonance · Point defects · Zircon

Introduction

To our knowledge, there has been but one survey of zircon spectroscopic properties (including electron paramagnetic resonance EPR), namely, the book

W. C. Tennant (✉) · R. F. C. Claridge · C. J. Walsby · N. S. Lees
Department of Chemistry, University of Canterbury,
Private Bag 4800, Christchurch, New Zealand
e-mail: C.Tennant@it.canterbury.ac.nz
Tel.: +64-3-364-2987 ext 7414
Fax: +64-3-364-2110

Present address: C. J. Walsby · N. S. Lees
Department of Chemistry,
Northwestern University, Evanston, IL 60208, USA

Spectroscopy of zircons; *properties and geological applications* (in Russian) by Krasnobaev et al. (1988). This book is referred to frequently in this article and we shall normally, after any reference to it, give a specific page and/or figure reference in brackets as follows (KVK88, p. 81, Fig. 52, for example). The book contains an extensive description and bibliography of the literature up to 1988 and includes EPR, optical absorption, thermo-, electro- and photoluminescence spectral studies of zircon. In part, the present article is aimed at making some of this information available to a wider audience. The reader is referred also to a general review article by Marfunin (1974a) and three general texts on magnetic, optical and luminescence spectra of minerals by the same author (1974b, 1975, 1979) and another by Vinokurov (1974). These latter references are not specific to zircon.

In this article we shall deal almost exclusively with EPR spectroscopy. We shall endeavour in the review section to cover the literature for the period 1960–2002. We take the opportunity also to present considerable, previously unpublished, data on zircon EPR from our own laboratory (Walsby 1999; Lees 2001).

The study, principally by EPR, of crystalline zircon (zirconium silicate) is of interest and importance for several reasons. From the structural standpoint zircon represents an interesting crystalline system that is intermediate between the purely ionic crystals such as alkali halides, and molecular crystals such as silicon dioxide (quartz). In zircon the cation Zr^{4+} is ionically linked to SiO_4^{4-} units within which the bonding can be regarded as essentially covalent (Fig. 1). From the technological viewpoint, zircon, or materials with the zircon structure, have been used as television phosphors (Thorpe et al. 1977). There has been some interest also (Abraham et al. 1969 and Ball 1982) in high-purity zircon as a possible lasing material. In these cases it is important to be aware of the impurities, often at trace levels, which may be associated with unpaired electrons and consequently be amenable to study by EPR. The inherent hardness, resistance to
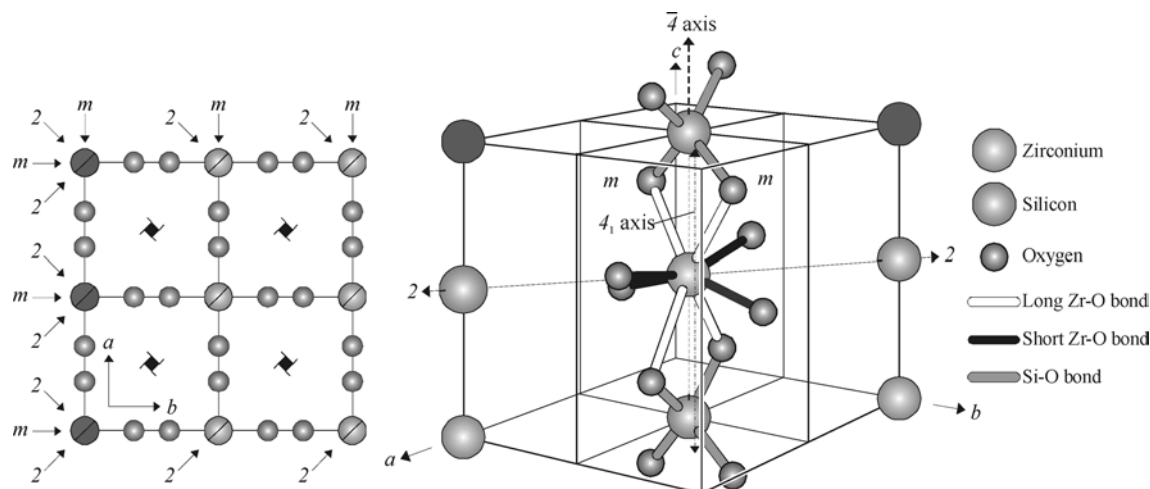
Fig. 1 Portion of the zircon unit cell showing interconnection of SiO_4^{4-} tetrahedra and Zr^{4+} ions along the $\bar{4}$ axis (*right*) and zircon structure when viewed along the *c* axis (*left*)

chemical attack and high refractive index are properties of zircon that enhance its use as a possible high-tech material in, for example, "solid-state and fast scintillation devices" (Abraham et al. 1969).

We shall order this article from several standpoints. First, we detail the crystal structure of zircon and consider in some detail the ramifications, from the point of view of EPR spectroscopy, of impurity substitution in one of the lattice sites. Second, we consider electron removal or electron addition to a normal atom, or to a substitutional ion in a lattice position, or vacancy defects. Next, we shall attempt to systematise the subject in terms of either electron-trap centres – usually traps associated with first or second-row transition ions or rare-earth ions – or electron-deficient (hole) centres. These latter are, in all cases thus far observed, centres in which an electron has been lost from one of the ligand oxygen atoms as a result of irradiation.

For completeness, one should include in such a review a description of the principal technique EPR as applied to crystals for the benefit of non-specialists who may wish to use the data and results presented. The reader is referred rather to the texts Abragam and Bleaney (1970), Weil et al. (1994) and the excellent section *Electron paramagnetic resonance in crystals* contained in a review of electron spin resonance studies of paramagnetic defects in crystalline quartz by Weil (1984), and general references therein. We shall, however, give a brief coverage of the spin-Hamiltonian (SH) and its use in analysing some of the paramagnetic centres to be discussed later in the review.

It will be necessary to consider in considerable detail the symmetry aspects of the study of crystalline zircon in relation to EPR techniques used and the type of information available from these studies. We shall consider these aspects in the following section.

Zircon crystallography

Crystal structure

Zircon has been the subject of a number of X-ray structural determinations, the most recent being that of Hazen and Finger (1979). These authors determined the structure over a range of pressures, 1–48.1 kbar. Robinson et al. (1971) earlier detailed a 3-D X-ray structure and compared it to that of garnet. This reference also reviewed the earlier literature and listed papers by Vegard (1926), Binks (1926), Hassel (1926), Wykoff and Hendricks (1928), Krstanović (1958), White and Gibbs (1967) and Krstanović et al. (1968). In the discussion that follows we shall use almost exclusively the most recent data of Robinson et al. (1971) and the ambient pressure data of Hazen and Finger (1979); the structural details in these two cases agree very closely.

Zircon crystallises in the tetragonal space group $I4_1/amd$. SiO_4^{4-} units are ionically linked with Zr^{4+} ions as depicted in Fig. 1. Each of the Si and Zr ions in the structure has dodecahedral D_{2d} ($\bar{4}2m$) point-group symmetry. Each Si is surrounded by four covalently bound O atoms at distances 166.2 pm (Robinson et al. 1971; Hazen and Finger 1979). These are slightly longer than the average of 161.2 pm found for α-quartz (Le Page et al. 1980), generally regarded as a purely covalent lattice. The SiO_4 tetrahedron has dodecahedral symmetry rather than regular tetrahedral; the observed symmetry of Si is thus D_{2d}. Each Zr^{4+} ion is surrounded by eight oxygens arranged in two distorted interleaving tetrahedra of long (226.8 pm) and short (213.1 pm) bonds. The geometry can be alternatively described as a triangular dodecahedron (Hoard and Silverton 1963) in accordance with the D_{2d} symmetry observed for the Zr^{4+} ion.

The structural units of zircon can be envisaged also as a chain of alternating edge-sharing SiO_4 tetrahedra and ZrO_8 triangular dodecahedra extending parallel to *c*, the four fold rotatory inversion axis of the zircon unit cell. The chains are joined laterally by edge-sharing dodeca-

hedra and are responsible for the prismatic habit of zircon. Robinson et al. (1971) point out that similar chains occur in cubic garnet, extending in three mutually perpendicular directions. They are linked, in this instance, by YO_6 octahedra (Y = typically a + 2 cation, Ca^{2+}, Mg^{2+}, Fe^{2+}) as well as by XO_8 dodecahedra (X = typically a + 3 cation, Al^{3+}, Fe^{3+}, Cr^{3+}, Mn^{3+}; Novak and Gibbs 1971). In zircon, octahedral voids are present but "contain no cations" (Robinson et al. 1971). (As discussed later in this article, the EPR evidence seems unequivocal also on this point: there is no direct EPR evidence of any occupation of the interstitial octahedral voids). The structural similarities of zircon and garnet are said to account for their similar hardness, density and high refractive indices (Robinson et al. 1971).

Symmetry aspects

Crucial to a proper understanding of EPR spectra in crystalline environments is an appreciation of the relationships between the symmetry of the spin SH and the symmetry of the site of the paramagnetic ion. The principles involved from the point of view of crystal physics are not new and have been well described, for example, in the textbook by Nye (1957). The basic principle is that of Neumann: The symmetry elements of any physical property of a crystal must include the symmetry elements of the point group of the crystal. In the EPR experiment we can regard the experimentally determined parameter matrices as physical properties of the crystal and can thus expect Neumann's principle to apply, but here one can be more specific. The parameter matrices are properties of the *site* of the paramagnetic ion and the symmetry elements in question are those of the point group of the site. Some of the parameter matrices of the conventional SH map as second-rank tensor quantities for which a condition of crystal physics is a centre of symmetry – in addition to the symmetry elements of the point group of the site. A centre of symmetry is imposed on the SH by the requirements of time reversal invariance (McGavin and Tennant 1985). Thus, all sites of paramagnetic ions, from the EPR standpoint, exhibit a centre of symmetry whether or not the crystal is centrosymmetric.

In single-crystal EPR experiments one wants to know how the observed site splittings in the EPR spectra are related to site symmetry and how these can be best used to extract optimum values of the SH parameters. Two seminal papers by Rae (1969) and by Weil et al. (1973) (see also Weil 1973) detail the relationships between the number of species observable in given orientations of the magnetic field vector, **B**, and the point-group symmetries of the sites of the paramagnetic species. (The reader is referred also to papers by Nizamutdinov et al. (1973, 1976), that classify paramagnetic centres for all of the 230 space groups.) We shall now outline these principles with particular regard for the possibilities in zircon. For the moment, we shall deal only with paramagnetic ions

occupying lattice positions in the zircon unit cell. We shall make the assumption that any distortion (lattice relaxation) that takes place as a result of substitution or formation of a paramagnetic species does not alter the point-group symmetry of the site. In terms of the contents of the previous paragraph, this means that we regard distortion/relaxation as being also a physical property of the site of the paramagnetic ion. The situation can be altered, of course, by the presence of some foreign nearby ion that may be required for charge compensation.

In zircon, space-group symmetry tetragonal, $I4_1/amd$, the lattice positions are of two types: Si and Zr positions (four of each per unit cell with Wyckoff designations a and b) each of which lies on the $\bar{4}$ rotatory inversion axis of the zircon unit cell and has $\bar{4}2m$ (D_{2d}) point-group symmetry: and the ligand oxygens, 16 per unit cell with Wyckoff letter designation h, each lying in one of the mirror planes of the zircon structure. Each O therefore has point-group symmetry m (C_s). The most common symmetries that one might expect to be reflected in the EPR parameter matrices of paramagnetic centres in zircon are the point groups $\bar{4}2m$ for tetragonal Si or Zr centres, or m for centres on an oxygen atom (or an Si or Zr centre interacting with another Si or Zr position along either the c or twofold axis). Strictly, because of the imposed centre of symmetry, one is concerned with the Laue class (point-group symmetry + a centre of inversion) of the site of the paramagnetic centre (see Rae 1969 and Weil et al. 1973 for further detail). Consequently 4 / mmm (D_{4h}) Laue class is observed for the tetragonal centres, at a Zr or Si atom position, and $2/m$ (C_{2h}) Laue class for most centres on O (or associated with O). The EPR experiment alone cannot distinguish, in the zircon case, the tetragonal point groups 422 (D_4), 4 mm (C_{4v}), $\bar{4}2m$ (D_{2d}) or $4/mmm$ (D_{4h}) but $\bar{4}2m$ point-group symmetry can be inferred from the known space group of the crystal and the sites available for electron capture/loss or for substitution. Similarly EPR spectra alone do not distinguish between the point groups 2 (C_2) or m (C_s) (or indeed $2/m$ (C_{2h}), assuming this point-group symmetry were possible) but comparison of principal directions of interaction matrices with symmetry axes of sites with known symmetry axes can lead to an unambiguous determination of the point-group symmetry.

The two point-group symmetries, $\bar{4}2m$ and m are indeed observed in the majority of the centres reported from single-crystal EPR measurements of centres in zircon. However, there are reported cases where the point-group symmetry of the paramagnetic species is other than the above two, namely, 2 (C_2), $mm2$ (C_{2v}), and 1 (C_1) and we now consider briefly how these might arise. Point-group symmetry 2 can be inferred if one principal direction of all interaction matrices lies along a crystal two fold axis. In zircon this implies one of the two dihedral two fold axes. Such a case might be two species, such as an electron centre and a compensator, lying on the same dihedral axis. Paramagnetic species with point-group symmetry m can be distinguished readily because the inherent two fold axis containing one

principal direction of all interaction matrices lies perpendicular to the mirror plane containing the species and no principal direction can lie simultaneously along a dihedral two fold direction. Paramagnetic species with no symmetry other than a centre of inversion, $\bar{1}$ Laue class (C_i), can arise as follows: (1) a paramagnetic species located in a general (interstitial) position; (2) a paramagnetic species located in a lattice position but interacting with a second ion in a general position; (3) a paramagnetic species located in a lattice position interacting with a second ion also in a lattice position but located in a distinct mirror plane. Examples are rarely reported and it is difficult to distinguish the three cases. Orthorhombic site symmetry, specifically point-group symmetry $mm2$, is in principle available in the space group of zircon (Henry and Lonsdale 1969, International crystallographic tables, vol I). It might arise from a paramagnetic species sitting on one of the four fold rotatory inversion axes where for some reason the Zr and/or Si atoms are displaced or missing from their normal lattice positions. It could arise also when two defect species, substituting ions or vacancies, occur at the adjacent Si/Zr lattice positions along the c axis. Again, reported examples are rare.

Definitive determination of the point-group symmetry of the paramagnetic species requires observation of site splittings in known planes of measurement. An early paper by Rae (1969) established the relationships amongst the Laue symmetry of the species, the Laue symmetry of the crystal and the number of species observable in specific crystal directions. Details are given for possible Laue site symmetries for each of the 11 Laue crystal classes. Implicit in this paper, as detailed by Weil et al. (1973) and Weil (1973), are the relationships amongst the observed site splittings and 3×3 proper rotation matrices $\mathbf{R}_i$ which relate the symmetry-related tensors $\mathbf{Y}_i$ associated with a given tensor $\mathbf{Y}$ via the similarity transformation

$$\mathbf{Y}_i = \mathbf{R}_i \cdot \mathbf{Y} \cdot \mathbf{R}_i^{-1} \; . \tag{1}$$

All proper rotation matrices for each of the 11 Laue crystal classes are listed. Weil et al. (1973) also listed the conditions under which a given parameter matrix can be completely determined from measurements in fewer than three distinct planes using the symmetry-related sites. Knowledge of the proper rotation matrices $\mathbf{R}_i$ appropriate to the site point-group symmetry is assumed.

We now consider the possible site splittings for each of the available Laue site classes for the specific case of the zircon crystal. From Weil et al. (1973) the proper rotation group appropriate to Laue crystal class $4/mmm$ is D_4 and there are eight associated proper rotation matrices $\mathbf{R}_i$ ($I = 1$–8). Thus, the EPR spectrum of a paramagnetic ion in a site containing only inversion symmetry would be expected, in a general crystal orientation, to exhibit eight symmetry-related species. In practice, provided measurements are restricted to planes containing two crystallographic axes, the maximum number of species observed is four and one can utilise the four rotation

matrices of the proper rotation group C_4 (see Claridge et al. 1994a,b). For a site of Laue class $2/m$ one finds then a maximum of four symmetry-related species, but in principal crystallographic planes this is reduced to 3 or 2, depending on the plane of measurement. From Rae (1969) one can, by observation of site splittings in given planes of measurement, determine whether the Laue class is $2/m^2$ or $2/m^3$ ($2/m^1$ is not possible in zircon) where superscripts 1, 2, 3 refer to the primary, secondary and tertiary axes, respectively, of the tetragonal system. The two fold (or inherent two fold) axis is easily identified from such observations and the point group established as either m or 2 by reference to the unit-cell structure. A maximum of two symmetry-related species in any arbitrary orientation, with each two fold (strictly four fold) degenerate, establishes the site symmetry as Laue class mmm. Observation of a single species in all crystal orientations establishes the spectrum immediately as tetragonal with the paramagnetic species occupying probably either of the Si or Zr positions – without compensation, stabilisation or magnetic interaction from a neighbouring ion.

This section on symmetry would not be complete without some mention of the possibility of Jahn–Teller distortions. We refer to the specific cases of certain d^1 ions, Zr^{3+}, Ti^{3+}, V^{4+}, Cr^{5+}, Nb^{4+} which are known to form paramagnetic centres in zircon and which are produced as a result of irradiation or substitution followed by irradiation. Of these ions, only V^{4+} has been studied in any detail from the point of view of the Jahn–Teller effect (Ball and Lowther 1977; Di Gregorio et al. 1982). Similar considerations should apply to the other ions. A strong Jahn–Teller coupling has been observed for Ti^{3+} in ZnSe (Dziesiaty et al. 1994). The situation in zircon depends on whether the ion, if an impurity, substitutes in the Zr or Si position in the lattice. Both have point-group symmetry D_{2d}, the former being considered as a distortion on eight fold cubic symmetry and the latter as a distortion on four fold cubic symmetry. A simple crystal-field analysis of the parameter matrices $\mathbf{g}$ and $\mathbf{A}$ in either case establishes unambiguously that the ground state wavefunction is $d_{x^2-y^2} \sim |b_1\rangle$ (or $d_{xy} \sim |b_2\rangle$, depending on choice of coordinates (Claridge et al. 1995; Lees, 2001)). From point-charge calculations (Fig. 2) the excited orbital states for Zr substitution are, in ascending order of energy, a doubly degenerate e-state $|e_a\rangle, |e_b\rangle$ (strictly degenerate only in the absence of spin-orbit coupling) some few thousand cm^{-1} above the ground state, $|a_1\rangle$ and $|b_2\rangle$. For Si substitution, the ordering above the $|b_1 >$ ground state is $|b_2 >$, $|a_1 >$ (or the reverse, depending on choice of parameters: Randic 1962; Kumar et al. 1980; Claridge et al. 1995; Lees 2001). The $|e >$ state is highest some 15 000 cm^{-1} above the ground state for Ti^{3+} substituting in the Si site. As illustrated in the point-charge calculations of Fig. 2 (Lees 2001), the energy levels for Ti substituting in the Zr or Si positions can be considered as distortions of a eight fold and four fold cube, respectively. One is interested in Jahn–Teller allowed distortions involving
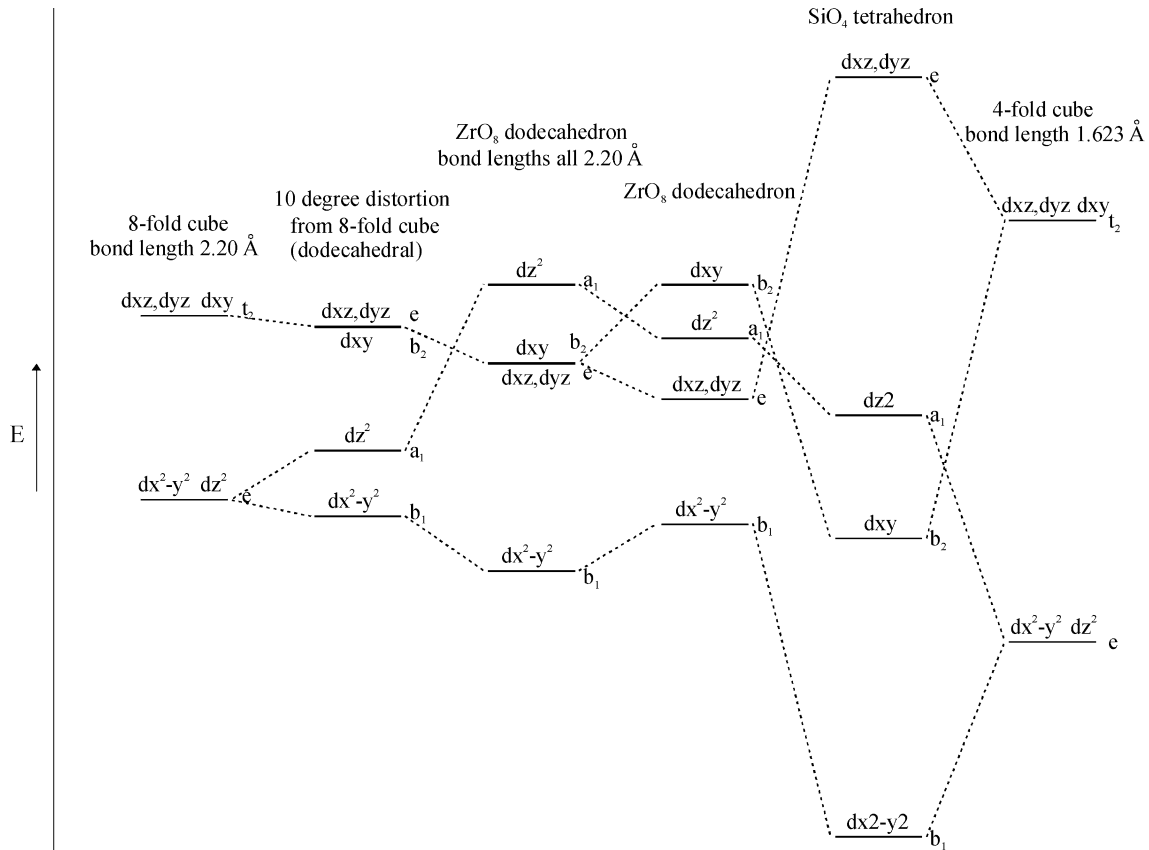
Fig. 2 Crystal-field splitting of 3d energy levels from point-charge calculations for various sites in zircon from Lees (2001). The labels on the right of the energy levels are the appropriate symmetry labels for the *d* orbitals

the degenerate *e*-orbitals. Since the symmetric square is $[E^2] = a_1 + b_1 + b_2$, we are interested in the coupling $E \otimes b_1$ (or $E \otimes b_2$). Any splitting derived from this effect is expected to be small in comparison with spin-orbit and crystal-field splittings. In the case of a d^1 ion in the Si site, one might be interested in the vibronic (dynamic) coupling of the ground $|b_1 >$ and low lying $|a_1 >$ states. As discussed by Di Gregorio et al. (1982), these states can be regarded as being derived from a tetragonal distortion of the ^2E state of a four coordinate cube (Di Gregorio et al. 1982). Several papers concerning JT effect are discussed later in this review.

Spin-Hamiltonian analysis of EPR single-crystal spectra

This section will serve to give the reader sufficient background to appreciate the papers to be included in this article and in particular to appreciate the notations in common use. It is not meant to be comprehensive or exclusive. The reader is referred to the minireview section *Electron paramagnetic resonance in crystals* contained in the review of EPR in crystalline quartz by Weil (1984) and to the standard texts, particularly Abragam and Bleaney (1970) and Weil et al. (1994).

For a paramagnetic ion with $S \leq 1$, $I \leq 1$, where S is the effective electron spin and I the nuclear spin, we shall write the SH for a single site as:

$$\mathscr{H}_S = \beta_e \mathbf{B}^T \bullet \bar{g} \bullet \mathbf{S} + \mathbf{S}^T \bullet \bar{D} \bullet \mathbf{S}$$
$$+ \sum_j \left\{ \mathbf{I}^T \bullet \bar{A}_j \bullet \mathbf{S} + \mathbf{I}^T \bullet \bar{P}_j \bullet \mathbf{I} - \beta_n \mathbf{B}^T \bullet (\bar{g}_n)_j \bullet \mathbf{I} \right\}.$$

$$(2)$$

In Eq. (2) **B**, **S** and **I** are (column) vectors representing the magnetic field, the effective electron spin and the nuclear spin, respectively; the superscript T represents transpose (i.e. $\mathbf{B}^T$ is a row vector) and the summation is over the $j = 1-n$ nuclei present. The symbols $\bar{g}$, $\bar{D}$, $\bar{A}$, $\bar{P}$ and $\bar{g}_n$ are 3×3-parameter matrices sometimes referred to as the electronic g, fine structure, hyperfine structure, nuclear electric quadrupole and nuclear g tensors, respectively. (In this review we shall avoid the term tensor. The parameter matrices $\bar{D}$ and $\bar{P}$ behave as second-rank traceless tensors, i.e. their diagonal elements sum to zero; the remaining three do not behave as true tensors – see Abragam and Bleaney 1970). Equation (2) is an SH representation of but one of the symmetry-related parameter matrices, the others being related by the appropriate proper rotation (Euler) matrices as discussed in the previous section. In all cases met in this review, the parameter matrices of Eq. (2) are assumed symmetric.

For sites with tetragonal symmetry the parameter matrices in diagonal form are simpler. For example,

writing $\bar{Y}$ for the g, A, and g_n parameter matrices and $\bar{Y}'$ for the traceless D and P matrices, we have the relations

$$Y_{xx} = Y_{yy} = Y_\perp \text{ and } Y_{zz} = Y_\parallel \tag{3a}$$

$$Y'_{xx} = Y'_{yy} = -Y'_{zz}/2 \; . \tag{3b}$$

For transition ions with S or $I \geq 3/2$, higher spin operators are required in the SH to describe adequately the EPR spectra. Most common in the literature are the so-called Stevens' operators (Pryce 1950; Abragam and Pryce 1951; Elliot and Stevens 1952; Stevens 1952), O_k^q ($-k \leq q \leq k$), which are combinations, chosen to have real coefficients, of equivalent operators related to spherical harmonic functions. Because such operators are not readily transformed using tabulated rotation matrix elements, it has become increasingly common to replace the Stevens' operators by spherical tensor operators $T_{k,q}(\mathbf{J})$, $\mathbf{J} = \mathbf{S}, \mathbf{I}$ (Kikuchi and Matarrese 1960; Buckmaster et al. 1972). It should be noted, however, that it is possible, via a spherical tensor form, to consistently transform the Stevens' operators (see Tennant 1976). Rudowicz (1985) has used such methods to produce a set of extended Stevens' operators along with matrix elements for a polar axis transformation. Particularly useful forms of tensor operators choose tesseral combinations of $T_{k,q}$ operators (McGavin and Tennant 1985; Tuszynski et al. 1985; Buckmaster and Chatterjee 1998). A set of such operators, designated $\mathfrak{I}_{k,q}$ by McGavin and Tennant (1985) and McGavin et al. (1990), have real coefficients, as do the Stevens' operators. (It is noted that the shorthand forms $T_{k,q}$ and $\mathfrak{I}_{k,q}$ are frequently employed). The O_k^q Stevens', and $\mathfrak{I}_{k,q}$ tesseral operators are related simply by a factor (see again the previous two references) and the rules for which combinations should be chosen to fully describe sites of given Laue class are also tabulated (McGavin and Tennant 1985; Tuszinski et al. 1985; McGavin 1987). As an illustration, the following terms would need to be added to Eq. (2) to describe adequately an ion with $S \leq 5/2$ in a site of $4/mmm$ Laue class

$$\mathscr{H}^{(4)} = B_4^0 O_4^0 + B_4^4 O_4^4 \tag{4a}$$

Or, equivalently

$$\mathscr{H}^{(4)} = B_{4,0} \mathfrak{I}_{4,0} + B_{4,4} \mathfrak{I}_{4,4} \; . \tag{4b}$$

Here $O_4^0 = 2\sqrt{70}\mathfrak{I}_{4,0}$ and $O_4^4 = 2\sqrt{2}\mathfrak{I}_{4,4}$ (see Table 1 of McGavin et al. 1990 for an extensive tabulation of such relations). In addition to the advantage of ease of transformation, the tesseral combinations of spherical tensor operators have the additional advantage that they are fully reduced and the SH expressed in their terms contains no more terms than are necessary (Grachëv 1987; McGavin et al. 1990; Tennant et al. 2000). This is not always the case for Stevens' and extended Stevens' operators (McGavin et al. 1990; Tennant et al. 2000). We shall meet both nomenclatures in papers covered in this review.

Zircon: crystal occurrence and crystal growth

Naturally occurring and synthetic crystals have been used extensively in EPR experimental work. Natural zircons occur widely in the Earth's crust and may contain a plethora of paramagnetic species as a result of impurity substitutional ions including transition ions of the first or second or third series, rare-earth ions and transuranic ions. In addition, natural radiation from various sources may have induced EPR active species. We shall discuss these aspects more fully in the next section.

The occurrence and geochemistry of zircon have been discussed generally in the textbook by Goldschmidt (1954). Heaman et al. (1990, and references therein) detail the minor and trace elements that are found in zircon fractions isolated from a variety of igneous rocks. Zircon grains crystallising in different magmatic environments are said to have unique geochemical signatures. A summary in Gorz (1974) records the presence of up to 50 minor and trace-element impurities in zircons; there can be profound differences in the abundance of some elements such as the rare-earth elements as well as Hf, Ta and Sc in zircons isolated from various magmatic sources.

Zircon single-crystal growth for research purposes is restricted mainly to either flux (Ballman and Laudise 1965; Chase and Osmer 1966) or hydrothermal growth (Frondel and Collette 1957; Dharmarajan et al. 1972; Uhrin et al. 1974). The earliest flux growth method for zircon dates back to 1888 (Hautefeuille and Perrey 1888, see also Frondel and Collette 1957). For EPR experiments, particularly where doping with various foreign ions may be required, the flux growth method described by Chase and Osmer (1966) has often been used, whereby the crystal is obtained from an equimolar mixture of ZrO_2 and Li_2SiO_3 (typically around 3 wt%) contained in a flux of molybdenum trioxide, MoO_3 and lithium molybdate, Li_2MoO_4. The melt is held at a temperature of around 1250 °C for a short period and then slowly cooled over several days Crystals as large as several mm in length are readily obtained. Doping ions may be incorporated readily by adding the appropriate metal oxides to the melt in suitable (low) concentrations. Ball and Wanklyn (1976) showed that additions of small amounts of PbO and Bi_2O_3 can often be useful in producing good well-formed crystals suitable for EPR experiments. Hydrothermal methods are stated (Uhrin et al. 1974) to be most advantageous for obtaining cm-sized zircon crystals.

Occurrence and production of paramagnetic centres in zircon

Both naturally occurring and synthetic zircons are known to contain stable EPR-observable paramagnetic centres arising from, for example, impurity ions in the

lattice, trapped radicals or electron holes or vacancies. In natural crystals some centres will have been produced by radiation, perhaps from a trapped radioactive nuclide (Strutt 1914; Fielding 1970; Eftaxias et al. 1989) or, more often, from a nearby radioactive mineral (Strutt 1914; Lietz 1937). In addition, further paramagnetic centres may be induced in either natural or synthetic crystals by irradiation with UV light (Lietz 1937), or X- or gamma radiation (Samoilovich et al. 1968; Vinokurov et al. 1971; Solntsev and Shcherbakova 1973a; Solntsev 1973, 1974; Marfunin 1974; Claridge et al. 1994a). A book by Meil'man and Samoilovich (1977) details EPR spectroscopy of activated single crystals. Laruhin et al. (2002) discussed the possibility of zircon being used as medium for luminescence dating. These authors used EPR to study paramagnetic centres produced by ionising radiation as a function of irradiation dose and annealing times to assess their feasibility as luminescence centres for dating purposes. Holland and Gottfried (1955) and Vaz and Senftle (1971) had earlier suggested the possibility of radiation dosimetry applications of zircons.

In the laboratory, irradiation must often be carried out at low temperature to produce the required centre (Samoilovich et al. 1968; Solntsev and Shcherbakova 1973a; Claridge et al. 1994a), and the stability of the centre may require that the temperature remain low. Thus, irradiation in situ is required or, alternatively, cold transfer to the EPR cavity (Claridge et al. 1994a) following irradiation. The stability of centres, particularly those induced by irradiation of the zircon crystal, varies widely. Some centres are annealed out on raising the temperature, while others remain stable to multiple annealings. In either case, it is possible that the centres may be observed only at temperatures approaching that of liquid helium (Solntsev and Shcherbakova 1973a; Claridge et al. 1994a). The stability of centres with respect to temperature or to power saturation can present problems for the EPR experimentalist. They can, however, be useful tools that allow one to systematically remove some paramagnetic centres that may interfere with the centre that is under study (Claridge et al 1994a; 1995).

Figure 3, an X-band c axis EPR spectrum at ca. 15 K, taken from Claridge et al. (1994a), will give some idea of the multiplicity of paramagnetic species observable by EPR. The crystal is a nominally pure zircon crystal grown by the Chase and Osmer (1966) flux technique, X-irradiated at 77 K and transferred cold to the EPR cavity. From low field the labelled centres are briefly as follows: E is an Al^{3+}-compensated oxygenic-hole centre (Solntsev and Shcherbakova 1973a; Krasnobaev et al. (KVK88, p. 90, Fig. 55); Claridge et al. 1994b). D and F (designated RT later in this article) are further oxygenic-hole centres (Claridge et al 1994a,b). C is also an oxygenic-hole centre (Claridge et al. 1999b), stabilised by an adjacent Zr vacancy. Parallel to c, the C centre coincides with an electron trap centre, here labelled Z, which arises from an impurity

Cr^{3+} ion (Claridge et al. 1999b). B and A are also electron-trap centres, the former arising from an impurity Ti^{3+} ion (Solntsev and Shcherbakova 1973b; Claridge et al. 1995) and the latter from a Zr^{3+} centre. Both the B centre and the A centre, also known as $Zr(\alpha)$ (Solntsev and Shcherbakova 1973a), are formed when a lattice 4 + ion captures an electron during X-irradiation (Claridge et al. 2000a). We shall meet all of these centres in subsequent sections. Closer inspection of Fig. 3 shows that there are several other minor centres, some of which are also considered later.

Paramagnetic defects in crystalline zircon

We shall order this survey of EPR results on crystalline zircon as follows. Firstly, electron trap centres are discussed. These involve almost exclusively metal ion centres and we shall discuss them in their various periodic table series. Zr centres are treated first, and separately, since these centres alone are formed from electron capture at a lattice cation. Lastly we consider electron-deficient (mainly trapped-hole) centres.

Unless otherwise stated, hyperfine structure (hfs), fine structure (sometimes described by zero-field splitting, zfs, parameters) and nuclear electric quadrupole splittings will be given in units $1/g_e\beta_e$ G. Useful conversions are effected via the multipliers 10^{-1} (G $\rightarrow$ mT), 0.9348×10^{-4} (G $\rightarrow$ cm^{-1}) and 2.8025 (G $\rightarrow$ MHz). Uncertainties, where known, are given in parentheses following the parameter magnitude. Thus $g_{||} = 1.99994(2)$, $A_{||} = 27.54(6)$ G mean $g_{||} = 1.99994 \pm 0.00002$ and $A_{||} = 27.54 \pm 0.06$ G, respectively.

Electron-trap centres

Zr centres

The first report of EPR of Zr paramagnetic centres in zircon appears to be that of Solntsev and Shcherbakova (1973a). These authors studied gamma-irradiated zircons from natural deposits in the Urals and detected three separate paramagnetic Zr^{3+} centres at 77 K. The centres were labelled $Zr^{3+}(\alpha)$ (parameters: $g_x = 1.882$, $g_y = 1.923$, $g_z = 1.934$; $A_x = 87.4$ G, $A_y = 50.0$ G, $A_z = 48.2$ G), $Zr^{3+}(\beta)$ (parameters: $g_x = 1.874$, $g_y = 1.913$, $g_z = 1.977$; $A_x = 79.8$ G, $A_y = 53.0$ G, $A_z = 24.6$ G) and $Zr^{3+}(\gamma)$ ($g = 1.897$; $A = 82.3$ G; only a g and an A factor quoted for this species). In each case the spectra are thought to arise from electron capture by a Zr^{4+} in a normal lattice position. From the quoted site splittings (maximum four in each case), the symmetry of the site must, however, be lowered from $\bar{4}2m$ (D_{2d}) to m (C_s) for each, implying interaction with a nearby ion lying in one of the mirror planes. Only in the case of the $Zr^{3+}(\gamma)$ spectrum from a crystal high in yttrium, was any EPR evidence of a foreign ion found: hfs from two
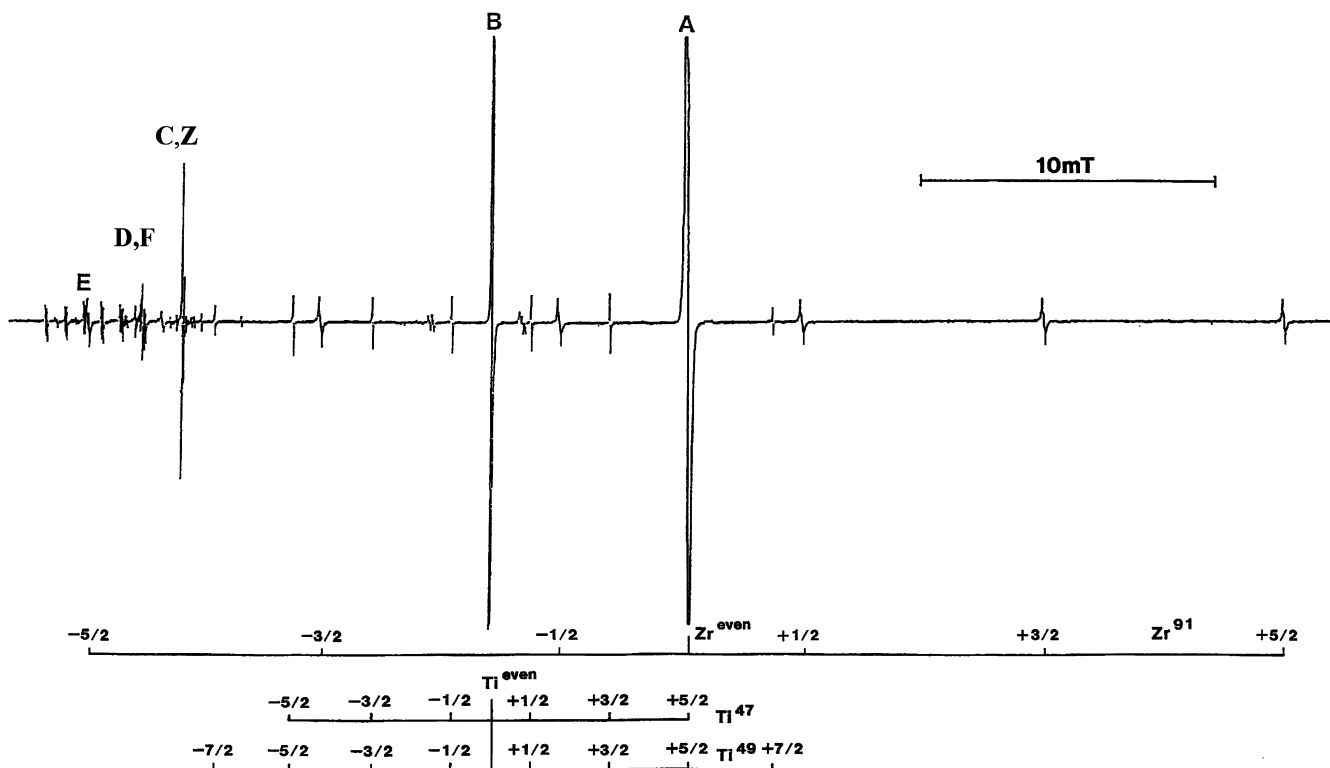
Fig. 3 15-K X-band spectrum, $\mathbf{B}||c$, of a nominally pure zircon crystal X-irradiated at 77 K. For details see text

equivalent 100% $I = 1/2$ nuclei in this instance. Gramolin (1981) also found three separate Zr^{3+} centres (along with an Hf^{3+} centre) in mixed crystals of zircon and xenotime (YPO_4) that is isomorphous with zircon. $Zr^{4+} \rightarrow Y^{3+}$ isomorphism and associated charge compensation in zircon has been discussed by Vinokurov et al. (1971). Samatov et al. (1983) also observed three structurally inequivalent Zr^{3+} complexes in xenotime. Abraham et al. (1984) studied ^{91}Zr enriched Zr^{3+} EPR spectra in xenotime. A colour centre in zircon, proposed by Matumura and Koga (1962, 1963) to arise from Zr^{2+} formed by gamma irradiation, has been subsequently shown by Barker and Hutton (1973) to be a hole centre.

Claridge et al. (1994a) studied the $Zr^{3+}(\alpha)$ centre further by X-band EPR at ca. 10 K. It was formed by X-irradiation at 77 K and identified, from its measured g values and hfs, to be the same centre as that of Solntsev and Shcherbakova (1973a). The measurements of Claridge et al. (1994a) were about order of magnitude more precise than those of Solntsev and Shcherbakova. Claridge et al. identified super hfs from a nearby 100% abundant $I = 1/2$ nucleus and fitted the spectra, including ^{89}Y hfs, to the SH, Eq. (2). The site point-group symmetry appeared slightly lower than m and a further, EPR-silent, interacting ion was inferred. Later, the same authors, Claridge et al. (2000a), remeasured the $Zr^{3+}(\alpha)$ spectrum ensuring very precise crystal alignment. The super hfs was measured very precisely using single-crystal EPR supplemented by ENDOR

(electron nuclear double resonance) measurements at the University of Paderborn, Germany. These studies established, unequivocally, the following: (1) the point-group symmetry of the site is m. (2) The observed super hfs arises from ^{31}P and not ^{89}Y as previously assumed (the ENDOR measurements together with the use of the appropriate g_n value for ^{31}P in the fitting made this assignment unequivocal). (3) The fitted hyperfine principal directions establish that the P is situated in an adjacent Si lattice position and (4) the g and A (^{91}Zr)-interaction matrices are, as expected of an ion in m point-group symmetry, non-coaxial. The principal values for this centre are: $g_1 = 1.93353(1)$, $g_2 = 1.92495(1)$, $g_3 = 1.883043(4)$; $A_1 = 87.831(5)$ G, $A_2 = 48.88(1)$ G, $A_3 = 48.03(1)$ G; $P_1 = 0.79(2)$ G, $P_2 = 0.41(1)$ G, $P_3 = -1.204(7)$ G. ^{31}P ($I = 1/2$, 100%) and ^{29}Si ($I = 1/2$, 4.67%) super hyperfine parameter matrices, obtained from ENDOR measurements, are detailed in Table 2 of Claridge et al. (2000a). The observation that ^{31}P might be an interacting 100% $I = 1/2$ nucleus in Zr^{3+} centres seems first to have been suggested by Gramolin (1981) (note title only abstracted in English). It seems that Solntsev (1973) also may have attributed super hfs in Zr^{3+} centres to ^{31}P (see Krasnobaev et al., KVK88, p.20).

First transition series – $3d^n$ ions

EPR of first long row elements in zircon is restricted, apparently, to those of the first transition series and then almost entirely to those ions with less than half-filled $3d$ shells. The elements Co, Ni and Cu in one of their known

higher oxidation forms ($+3$, $+4$) appeal as possibilities for forming electron-trap centres but, apart from brief mention of the first two by Krasnobaev et al. (KVK88, p. 66), no paramagnetic centres of these elements have been reported in zircon. Any scandium impurity would be expected to exist as diamagnetic Sc^{3+}. Additionally, to our knowledge, hfs from ^{45}Sc ($I = 7/2$, 100%) has not been observed in zircon. In what follows in this section we therefore restrict discussion almost entirely to paramagnetic electron-trap centres formed by the elements Ti to Fe – atomic numbers 22–26.

The first report of EPR of a Ti^{3+} (d^1) centre in zircon is that of Solntsev and Shcherbakova (1973b). (An earlier report by Samoilovich et al. 1968 appears to have wrongly ascribed observed resonances to Ti^{3+}; Solntsev and Shcherbakova 1973b). Analysis of the g and A values by a simple crystal field model showed that the ground state was $d_{x^2-y^2}(b_1)$ (or $d_{xy}(b_2)$ depending on choice of coordinates). In Ti^{3+} centres in α-quartz, on the other hand, the ground state is invariably d_{z^2} (Isoya et al. 1988). Claridge et al. (1995) reexamined the same Ti^{3+} centre by X-band EPR at ca. 10 K. Their quoted g values, $g_{||} = 1.92683(1)$, $g_{\perp} = 1.94067(1)$ correspond to those given by Solntsev and Shcherbakova (1973b). A more precise crystal-field analysis by Claridge et al. (1995), together with point-charge calculations on both the Si and Zr sites of the ideal lattice, showed that (1) the ground state is indeed $d_{x^2-y^2}$ (or d_{xy}) and, (2) Ti almost certainly substitutes for Zr in the lattice. The designation $[TiO_8]^-$ was proposed. In this paper there was also an indication that adequate analysis of the nuclear hfs of the ^{47}Ti (7.4%, $I = 5/2$) and ^{49}Ti (5.4%, $I = 7/2$) required higher spin terms of dimension BI^3, BI^7 in the SH. Verification of these latter proposals required measurements. of high precision, particularly in the crystal ab plane, where all second-rank parameter matrices are isotropic (for uniaxial symmetry), and with greatly improved sensitivity to study adequately all the many forbidden hyperfine lines involved. This work was reported in a further 10-K X-band EPR study by Claridge and Tennant (1997) and Tennant and Claridge (1999). Features of the spectra were: a marked $\cos 4\theta$ angular dependence of both the overall intensities and hyperfine line positions, particularly those of the ^{49}Ti isotope, in the ab plane of the crystal where isotropy would be expected for Ti^{3+} substituting for either of Zr or Si. In order to analyse the observed hfs, the SH, Eq. (2), was extended to include terms of dimension BI^3, BI^5 as well as terms of dimension SI^3, SI^5 and I^4. All produced fitted parameters that were statistically significant and which allowed an excellent fit of the angular dependence of the hyperfine lines in the ab plane. Figure 2, 3 and 4 of Tennant and Claridge (1999) illustrate the analysis for the ^{49}Ti isotope. Particular features of this work were that inclusion of all terms SI^k ($k = 1, 3, 5$) are necessary to describe adequately the nuclear hyperfine and nuclear electric quadrupole interactions and, similarly, all terms of dimension BI^k ($k = 1, 3, 5$) are necessary to describe adequately the nuclear Zeeman interaction. For example, for the latter interaction, a marked anisotropy was detected in the nuclear Zeeman interaction only when all BI^k terms were included in the SH analysis; this anisotropy could be identified with anisotropy in the chemical-shielding matrix (tensor). The reader is referred to the original papers (Claridge et al. 1995 and Tennant and Claridge 1999) for further details.

Two further Ti^{3+} centres, studied at X band at ca. 10 K, have been reported (Claridge et al. 1997a, 1999a). In both, Ti substitutes for Zr but each exhibits in addition super hfs from a nearby 100% $I = 1/2$ nucleus. The first of these was originally designated $[TiO_8/Y]^-$ (total charge 2- after taking Y^{3+} into account) with g values 1.954636(7), 1.945894(9), 1.914495(5). A distant unidentified cation was proposed to account for charge balance. Walsby (1999) later demonstrated that the hyperfine data could be fitted equally well with the g_n of either ^{89}Y or ^{31}P, the latter being favoured because it leads to the designation of a neutral cluster $[TiO_8/P]^0$. One principal direction of the hfs parameter matrix is directed towards a nearest-neighbour Zr or, alternatively, a nearest neighbour Si suggesting either Y substitution in the former or P substitution in the latter. Point-group symmetry m necessarily follows in either case. The second centre (Claridge et al. 1999a), with g values 1.963878(3), 1.936005(5), 1.912587(3), seems almost certainly, from the observed super hfs, to arise from Ti^{3+} in a Zr site interacting with a ^{31}P nucleus situated in a next-nearest-neighbour silicon position. In this case both Ti and P lie on one of the dihedral two fold axes of the zircon unit cell, explaining the coincidence of one g principal direction and one ^{31}P principal A direction lying along this crystal direction. The point-group symmetry of the Ti^{3+} in this instance is thus 2 (C_2). The designation $[TiO_8/P]^-$ has been suggested (Claridge et al. 1999a) but, as discussed above, taking the charge of the compensator into account, $[TiO_8/P]^0$ can be considered a more useful description (Walsby 1999). Krasnobaev et al. (KVK88, p. 85) reported a Ti^{3+} centre, designated $(Ti^{3+})_\beta$, which also displayed super hfs from a 100% $I = 1/2$ nucleus, in zircon. The quoted g values are 1.874, 1.993, 1.938, and the symmetry C_2. The g value magnitudes correspond only very approximately to those for a uniaxial centre that Claridge et al. (1999a) attribute to Ti substituting for Si in the zircon lattice (this centre is outlined in more detail below). Nevertheless, the C_2 point-group symmetry of the centre and the super hfs would be understandable if Ti substitutes for Si and the Ti^{3+} paramagnetic centre interacts with an $I = 1/2$ nucleus situated in a next-nearest-neighbour position along the dihedral two fold axis. That is, both Ti and the compensator lie on the [1 1 0] axis. We note en passant that no H- or Li-compensated Ti^{3+} centres similar to those observed in α-quartz (Rinneberg and Weil 1972; Isoya et al. 1988; Bailey and Weil 1992) have been observed thus far in zircon. This may be due to the different synthetic routes followed, namely, hydrothermal for quartz and (mainly) flux

growth for zircon, coupled with the lack of large interstitial channels in zircon.

The centres reported in the previous paragraph were studied in a nominally pure crystal following X-irradiation at 77 K and cold transfer to the EPR cavity. In a further study, using again X-band EPR at a nominal temperature of 10 K and a crystal deliberately doped with Ti, a new Ti^{3+} centre was observed (Claridge et al. 1999a). A crystal-field analysis, together with point-charge calculations, indicated Ti^{3+} substituting for Si in the lattice; the designation $[TiO_4]^-$ was suggested. The g values for this centre are: $g_{||} = 1.83617(2)$, $g_\perp = 1.98055(2)$, which as noted above, correspond in magnitude roughly to those for the lower symmetry centre reported by Krasnobaev et al. (KVK88, p. 85). A further uniaxial Ti^{3+} centre was reported in Krasnobaev et al. (KVK88, p. 16) with g values: $g_{||} = 1.876$, $g_\perp = 1.943$; no hfs was reported. The g values do not seem to correspond to any of the other centres thus far characterised.

EPR spectra of vanadium as V^{4+} have been observed and studied at temperatures below 20 K by Ball and Wanklyn (1976), Ball and Lowther (1977) and Di Gregorio et al. (1982). The Ball and Wanklyn data at 20 K are: $g_{||} = 1.8930(5)$, $g_\perp = 1.9699(5)$, and for the ^{51}V ($I = 5/2$, 100%), $A_{||} = 87.3(2)$ G, $A_\perp = 30.9(2)$ G. Ball and Wanklyn (1976) assumed that the V^{4+} ion substitutes for Zr in the zircon lattice. Ball and Lowther (1977) accounted for the temperature dependence of the g values between 4.2 and 20 K and an anomalously small hyperfine field as being due to a dynamic Jahn–Teller distortion – a vibronic coupling between the $^2b_1$ ($d_{x^2-y^2}$) ground state and vibronic states with ^2e representations. Di Gregorio et al. (1982) in an optical and EPR study of V^{4+} in zircon and three other zircon-type lattices argued from a crystal-field model and from point-charge calculations that the impurity ion occupies an Si dodecahedral site in the lattice. Using a superposition model to analyse optical absorption results, Xiaoyu et al. (1985) reached a similar conclusion. Beltrán et al. (1993) on the other hand, from ab initio cluster-in-the-lattice calculations, concluded that Zr replacement by V^{4+} is a more stable state than that of Si replacement; Jahn–Teller distortion had yet, however, to be considered. Di Gregorio et al. (1982) also analysed their EPR and optical results in terms of a dynamic Jahn–Teller distortion by considering the sites in each case as a small tetragonal distortion from four fold cubic symmetry. We note that occupation of the Zr site would require an approximation where the site symmetry would be considered a tetragonal distortion of eight fold cubic symmetry. Unfortunately, in contrast to the Ti^{3+} case, there appears to be only one type of V^{4+} EPR spectrum observed, so that there remains some doubt as to the actual site of V^{4+}.

EPR of Cr in zircon is the subject of two papers referred to in Krasnobaev et al. (KVK88, p. 61). A species with $g_{||} = 1.986$, $g_\perp = 1.956$ with $A \approx 10$–14 G is proposed to arise from Cr^{5+} (d^1). The green coloration of the crystals is said to be typical of Cr^{5+} in tetrahedral coordination. Greenblatt et al. (1981) reported EPR spectra of Cr^{5+} in YPO_4 and YVO_4, both with the zircon structure. In YPO_4, for example, where the lattice parameters are quite close to those of the isomorphous zircon structure, the EPR parameters for Cr^{5+} are: $g_{||} = 1.9772(5)$, $g_\perp = 1.9525(5)$, $A_{||} = 9.1(1.1)$ G, $A_\perp = 21.0(5)$ G; super hfs parameters from ^{91}Y are also reported. These authors propose that the results are explained by assuming a d_{z^2} ground state for the d^1 ion that arises from strong covalent contributions when Cr replaces Y in the lattice; point-charge calculations indicate the ground state for both Zr and Si sites under D_{2d} symmetry is $d_{x^2-y^2}$. The second report in Krasnobaev et al. (KVK88, p. 61) describes a Cr^{3+} (d^3) centre in which transitions from only the $m_s = -1/2 \rightarrow m_s = 1/2$ transition are seen. Hfs parameters are reported as $A_{||} = 19.2$ G, $A_\perp = 14.5$ G. No estimates of the zero-field splitting (zfs) parameters are given. From luminescence work on the same centre, Gaft et al. (2000) postulated that the centre is that of Cr^{3+} in a Zr site. Claridge et al. (1997b) observed two spectra at ca. 10 K in a nominally pure zircon crystal that had been X-irradiated. One of the species, $S = 1/2$, had an almost isotropic g matrix: $g_1 = 1.999386(2)$, $g_2 = 1.999373(3)$, $g_3 = 1.999243(1)$, while the second, $S = 3/2$, was extremely anisotropic with effective g matrix: $g_{||} \approx 2$ $g_\perp \approx 4$. The SH parameters for the $S = 3/2$ system were reported as: $g_1 = 1.9564(3)$, $g_2 = 1.9573(2)$, $g_3 = 1.9993(1)$ and $D = 4.5(9)$ T. From these results the spectra are, within error, coincident along the crystal c axis. These observations, together with microwave saturation experiments above 14 K, led the authors to speculate that the two centres may be coupled and the data were fitted satisfactorily to a spin triplet system with ferrimagnetic coupling constant $J = 24.4$ T. Subsequent experiments on various other synthetic crystals showed that the intensity ratio of isotropic to anisotropic centres was not constant and the microwave saturation behaviour between 4.2 and 14 K proved to be quite different for the two centres. They are consequently not coupled, and the anisotropic centre was shown unambiguously to arise from Cr^{3+}, probably substituting in a Si site (Claridge et al. 1999b). More precise 15-K X-band EPR studies on a synthetic crystal containing a higher concentration of the anisotropic centre confirmed it as Cr^{3+} (d^3) (Lees, 2001). From this study the SH parameters are: $g_{||} = 1.99924(4)$, $g_\perp = 1.95817(8)$; $|D| = 2.61(8)$ T and the hfs parameters for ^{53}Cr: $A_{||} = 15.75$ G, $A_\perp = 11.65$ G; super hfs parameters were also given for the ^{91}Zr nucleus. It should be noted that there is considerable uncertainty in the zfs constant D since measurements in only one of the two doublets of the spin quartet was possible. The doublet transition $m_s = -3/2 \rightarrow m_s = 3/2$ with effective g values $g_{||} = 6$, $g_\perp = 0$ (for very large zfs) is EPR-silent at X-band frequencies, although the zfs reported above predicts strong transitions at fields just outside the capabilities of the magnet used. A further centre, which corresponds in many respects to the Cr^{5+} centres

reported by Krasnobaev et al. (KVK88, p. 61) and Greenblatt et al. (1981), has been measured and partially characterised by Lees (2001). The g values for this centre are: $g_{||} = 1.98753(1)$, $g_\perp = 1.95503(1)$. However, there was considerable uncertainty in assigning lines that may arise from ^{53}Cr hfs and the actual designation of the species remains unclear. Belletti et al. (1995) used polarised absorption spectra and claimed that "... only the hypothesis of a replacement of Si^{4+} with Cr^{4+} is acceptable".

To our knowledge, well-resolved Mn^{2+} $S = 5/2$ (d^5) spectra have not been observed in zircon. In zircon doped with $MnSO_4$ Krasnobaev et al. (KVK88, p. 66) observed a broad isotropic line with $g = 2$ which may arise from Mn^{2+}. Reference to a possible Mn^{4+} $(d^3, S = 3/2)$ centre is given in Krasnobaev et al. (KVK88, p. 66) (see also Vinokurov 1974 and Meil'man and Samoilovich 1977) with reported parameters: $g_{||} = 2.008$, $g_{\perp} = 1.992$, and hfs parameters from a 100% abundant $I = 5/2$ nucleus: $A_{||} = 75$ G, $A_\perp = 53$ G. As with the Cr^{3+} centre reported above (KVK, p. 61, Claridge et al. 1999b), resonance was observed only in the $m_s = -1/2 \rightarrow m_s = 1/2$ doublet, the effective g values being $g_{||} \approx 2$, $g_\perp \approx 4$.

Fe^{3+} EPR in zircon has been the subject of papers by Vinokurov et al. (1972) and Ball and van Wyk (2000) (see also Vinokurov et al. 1974). Vinokurov et al. (1972) studied Fe^{3+} in natural non-irradiated crystals. The spectra were interpreted in terms of two different species, one arising from Fe^{3+} in the Si site and the other from Fe^{3+} in the Zr site. SH parameters given by Ball and Van Wyk (2000) are: $g_{iso} = 2.003(1)$, $B_2^0 = 1572(1)$ G, $B_4^0 = -0.209(1)$ G, $B_4^4 = -3.35(1)$ G for the first spectrum and $g_{iso} = 2.003(1)$, $B_2^0 = 821(1)$ G, $B_4^0 = 0.088(1)$ G, $B_4^4 = -0.86(1)$ G for the second spectrum. These parameters are substantially in agreement with the earlier study of Vinokurov et al. (1972), but Ball and van Wyk (2000) were unable to establish with reasonable certainty the sites of Fe. Possibilities considered were (1) Zr and Si replacement, (2) Zr replacement only, but with different charge compensators giving rise to distinct paramagnetic species (this seemed an unlikely possibility considering the factor of two between the magnitudes of the zfs constant D for the two species). As yet unpublished ab initio plane wave pseudopotential calculations by J.E.Lowther were stated to "not favour the replacement of Si^{4+} with Fe^{3+}", but were "inconclusive".

There are brief references to Ni^{2+}, Co^{2+} and Co^{3+} in Krasnobaev et al. (KVK88, p. 66) but no EPR parameters are given for any paramagnetic centre. Cu in any of its known oxidation states $+2$, $+3$, $+4$ does not seem to have been observed in zircon either optically or by EPR.

Second transition series – $4d^n$ ions

The introductory comments on the $3d$ series seem to apply also to the second long-row elements. EPR-active centres have been observed only for those elements with less than half-filled $4d$ shells. Y in its principal oxidation state $(+3)$ is, as for Sc, diamagnetic and does not apparently easily trap an electron to form an ion observable by EPR. However, Y is a common impurity in zircon and evidence of its presence is frequently observed via hfs from its $I = 1/2$, 100% abundant nucleus ^{89}Y. Again, In or Sn could, in principle, contribute indirectly to paramagnetic hole centres by acting as stabilising ions for trapped holes as do $+3$ ions of B, Al, Y in zircon (Claridge et al. 1994b, 2000b, Walsby et al. 2000) and Ga^{3+} in GeO_2 (Stapelbroek et al. 1977). Electron-trap centres for the $4d$ ions are next reviewed; Zr^{3+} centres have already been discussed.

EPR of $4d^1$ Nb^{4+} centres has been the subject of a number of studies. Nb is a common impurity in zirconium and Nb^{4+} can be expected to replace Zr^{4+} in zircon. Solntsev and Shcherbakova (1974) discussed mechanisms of charge compensation and the form of Nb and Y intrusions in the zircon structure. Vinokurov et al. (1963a) observed a spectrum at 77 K of ten equally intense and almost equally spaced lines that, moreover, did not exhibit site splitting in general crystal orientations. The lines were identified from the hfs of the 100% abundant $I = 9/2$ isotope ^{93}Nb. Fitted parameters were: $g_{||} = 1.862(1)$, $g_\perp = 1.908(1)$, $A_{||} = 309(3)$ G, $A_\perp = 138(3)$ G. A ground state similar to that of Ti^{3+} and V^{4+} $3d^1$ ions, namely, $d_{x^2-y^2}$, was inferred. Di Gregorio et al. (1980) studied the same spectrum also at 77 K and analysed the hyperfine data by a second-order perturbation approach. Their fitted g values, slightly modified as a result of second-order hyperfine corrections, were: $g_{||} = 1.822(5)$, $g_\perp = 1.895(5)$, $A_{||} = 309(1)$ G, $A_\perp = 141(1)$ G. These authors also presented a crystal-field analysis of the data from which a value of the hyperfine field at the Nb nucleus was obtained. Walsby (1999) carried out X-band EPR measurements at ca. 10 K on a ten-line spectrum identified from the data of Vinokurov et al. (1963a) and Di Gregorio et al. (1980) to be that of Nb^{4+}. Parameters were obtained by a full matrix diagonalisation procedure (Mombourquette et al. 1996). Included in the analysis were high-spin terms of dimension SI^k, BI^k, $(k = 3,5)$. A small diminution in the fitting errors was observed as a result of including these extra terms, but the magnitudes and their errors were of comparable size. In contrast to the situation found for the $I = 5/2$ ^{47}Ti and for the $I = 7/2$ ^{49}Ti isotopes of Ti (Claridge et al. 1995; Tennant and Claridge 1999), these terms are obviously unimportant. The fitted parameters for the conventional SH (Eq. 2) were: $g_{||} = 1.909010(7)$, $g_\perp = 1.862390(7)$, $A_{||} = -287.196(4)$ G, $A_\perp = -130.158(4)$ G, $P_{||} = -0.805(5)$ G, $P_\perp = 0.403(5)$ G. The signs of $A_{||}$ and $A_\perp$ were established as both negative from a crystal-field analysis of the principal g and A values; $P_{||}$ can be taken as negative, the same as that of the nuclear electric quadrupole moment for ^{93}Nb, provided the electric-field gradient is dominated by the valence contribution from the unpaired $4d$ electron.

Eftaxias et al. (1989) reported EPR of Mo^{5+} $4d^1$ from X-band measurements at around 15 K. The crystal used was a synthetic one produced from flux growth (Fielding 1970) and the Mo centre was observed following UV irradiation from a 150-W xenon lamp for 6 h at 15 K. The spectrum was stated, from the observed site splittings, to exhibit point-group symmetry 2 but within experimental error the SH parameters were orthorhombic. That is, the principal g and A values were, within error, coaxial and lay along the crystallographic axes. Quoted parameters were: $g_{xx} = 1.9256(3)$, $g_{yy} = 1.9372(3)$, $g_{zz} = 1.8863(3)$, $A_{xx} = 47.0(2)$ G, $A_{yy} = 45.7(2)$ G, $A_{zz} = 84.2(2)$ G. (The hyperfine principal values are from two isotopes with mass numbers 95, 97 each with $I = 5/2$ which are experimentally coincident because of their similar nuclear g values). The Mo^{5+} ion was thought to occupy a Si site in the crystal. Krasnobaev et al. (KVK88, p. 15) report two centres, attributed to Mo^{5+}, labelled $(Mo^{5+})_\alpha$ (uniaxial with parameters: $g_{||} = 1.877$, $g_\perp = 1.915$, $A_{||} = 86$ G, $A_\perp = 37.9$ G) and $(Mo^{3+})_\beta$ (rhombic with parameters: $g_{xx} = 1.867$, $g_{yy} = 1.944$, $g_{zz} = 1.861$, $A_{zz} = 86$ G).

A spectrum, tentatively ascribed to Ru^{7+} (also $4d^1$) with Li^+ compensator, has been reported by Krasnobaev et al. (KVK88, p. 19). The quoted parameters are: $g_x = 1.969$, $g_y = 1.981$, $g_z = 1.969$; from hfs (magnitudes in G) ascribed to ^{99}Ru ($I = 5/2$, 12.8%): $A_x = 3.9$, $A_y = 10.8$, $A_z = 17.2$, and to ^{101}Ru ($I = 5/2$, 17.0%): $A_x = 19.6$, $A_y = 39.2$, $A_z = 30.4$; A ^7Li hyperfine splitting of 0.5 G was given. Point-group symmetry C_{2v} is claimed for the species. The above evidence is convincing, but the authors note that the relative magnitudes of the two hfs sextets do not reflect the ratio of the nuclear g values, namely $g_n(101)/g_n(99) = 1.12$, so that the assignment to Ru must be suspect. Two centres for which the g value match is very close to the above centre have been measured by Lees (2001) and attributed to an electron centre interacting with either one or two B nuclei (see discussion below: Miscellaneous electron centres). The ion at which the unpaired electron resides is not known and the characterisation is incomplete.

Third transition series and rare-earth ions

Apart from the rare-earth ions, only Hf appears to have been observed by EPR. Hf, like Ti and Nb is a common impurity in zirconium; hafnon, $HfSiO_4$ is isomorphous with zircon. Hf EPR spectra would be expected to exhibit signature hfs from two of its isotopes, ^{177}Hf ($I = 7/2$, 18.6%) and ^{179}Hf ($I = 9/2$, 13.7%). An EPR spectrum of Hf^{3+} in hafnon, analogous to Zr^{3+} in irradiated zircon, may have been observed by Samoilovich et al. (1968) (see also KVK88, p. 69) and by Solntsev (1973): the first of these reported a uniaxial spectrum, $Hf^{3+}(\alpha)$ with parameters $g_{||} = 1.802$, $g_\perp = 1.992$, and the second a rhombic spectrum $Hf^{3+}(\beta)$ with parameters $g_{xx} = 1.802$, $g_{yy} = 1.880$, $g_{zz} = 1.998$; the lower symmetry arises apparently from the presence of a nearby stabilising ion Y^{3+} (see Vinokurov et al. 1971; Solntsev and Shcherbakova 1974). Samoilovich et al. (1968) reported hfs said to arise from ^{177}Hf and ^{179}Hf isotopes, but the nuclear spins are given erroneously as $I = 3/2$ in each case. Furthermore, the magnitudes given for the perpendicular factors, 7.8(1) G and 5.8(1) G, respectively, seem far too small (see the next entry). Also their ratio does not reflect very well the ratio of the nuclear g factors. In mixed crystals of hafnon and zircon $Zr_{1-x}Hf_xSiO_4$ with $x > 0.75$, a species said to be Hf^{3+} with nearby P^{5+} stabiliser is reported with parameters $g_{xx} = 1.892$, $g_{yy} = 1.922$, $g_{zz} = 1.935$; no Hf hfs is reported. A further uniaxial Hf^{3+}/Y^{3+} spectrum has been reported by Samatov and Votyakov (1983) (see also KVK88, p. 79 and Fig. 52) in xenotime with parameters: $g_{||} = 1.4032$, $g_\perp = 1.7323$; ^{177}Hf: $A_{||} = 178$ G, $A_\perp = 112$ G; ^{179}Hf: $A_{||} = 118$ G, $A_\perp = 80$ G. (The ratio $^{177}A_{||}/^{179}A_{||} = 1.51$ while the ratio of the corresponding g_n values is 1.59 in reasonable agreement).

EPR of the lanthanide series of $4f^n$ ions (the rare earths), where n may be either odd or even, are characterised by very large zfs that split the various spin multiplets (Kramers' doublets when n is odd) by 10–100 cm^{-1}. Generally, EPR is observable only in the lowest doublet. This doublet can be assigned a fictitious spin of 1/2 and the apparent g values are generally very anisotropic. The reader is referred to Abragam and Bleaney (1970) and to the original papers for further detail.

In addition to zircon, several authors, Nizamutdinov et al. (1974), Samatov et al. (1982) and Samatov and Votyakov (1983), have studied EPR of rare-earth ions in xenotime. The first-named authors reported EPR and spin-lattice relaxation of Nd^{3+}, Er^{3+}, Tb^{3+} and Dy^{3+} in a single crystal of xenotime.

An EPR spectrum of the $4f^1$ ion Ce^{3+} does not seem to have been observed in zircon. The rather large crystal ionic radius of Ce^{3+}, 103.4 pm, makes it an unlikely replacement for Zr in the lattice.

Harris et al. (1984) report 9.9 GHz EPR experiments at 15 K on a synthetic zircon crystal containing Pr. The observed spectrum is attributed to Pr^{4+} which has the configuration $4f^1$, a ^2F (free ion) state. Hfs from the ^{141}Pr nucleus ($I = 5/2$, 100%) was also measured. Matrix diagonalisation of the SH matrix from an SH of the form of Eq. (2) produced the following parameters for a spin system with $S_{eff} = 1/2$, $I = 5/2$: $g_{||} = 1.0038(2)$, $g_\perp = 1.0384(10)$, $A_{||} = 646.7(3)$ G, $A_\perp = 683.1(15)$ G. The results are discussed in terms of a $^2F_{5/2}$ ground state with small admixture of $^2F_{7/2}$ excited state. From only two effective g values a unique calculation of the zero-field splitting between the two levels was not possible.

Q-band EPR spectra of Nd^{3+} ($4f^3$) at 19 K have been reported by Ball (1982) in zircon and also in hafnon. Complete fingerprinting was possible from the observation of hfs from two isotopes ^{143}Nd ($I = 7/2$, 12.2%) and ^{145}Nd ($I = 7/2$, 8.3%). The spectra were uniaxial in both cases, as evidenced by position invariance in the crystal ab plane and absence of site splitting, with

parameters for zircon: $g_\parallel = 0.26(4)$, $g_\perp = 2.6486(4)$, ^{143}Nd $A_\parallel = 29(7)$ G, $A_\perp = 310.4(4)$ G, ^{145}Nd $A_\parallel = 19(5)$ G, $A_\perp = 192.8(3)$. Because the resonant field corresponding to $g_\parallel$ was beyond the upper range of the magnet, $g_\parallel$ had to be estimated by fitting data from a limited angular range in the crystal ac plane. The g values were analysed in terms of possible ground-state wavefunctions in a tetragonal field and two possible solutions given for an isolated Kramers' doublet of the form $a|\pm 9/2\rangle + b|\pm 1/2\rangle + c|\mp 7/2\rangle$. Again assuming an isolated doublet, the following relations were seen to be approximately true:

$$g^2 = g_\parallel^2 \cos^2\theta + g_\perp^2 \sin^2\theta$$

$$A^2 g^2 = A_\parallel^2 g_\parallel^2 \cos^2\theta + A_\perp^2 g_\perp^2 \sin^2\theta$$

$$g_\parallel / g_\perp = A_\parallel / A_\perp .$$

Kumar et al. (1980) have published crystal-field analyses of Nd^{3+} in compounds with the zircon structure.

Fielding (1969, 1970) reported observation of colour centres in zircon arising from Eu^{3+}. According to Abragam and Bleaney (1970) for the $4f^6$, $^7F_0$ ($S = 3$, $L = 3$, ground state $J = 0$) of Eu^{3+}: "Obviously, no EPR can be expected for an ion with $J = 0$". As described in the following paragraph, Eu^{2+} is one of a group of three transition metal ions with a half-filled $4f$ shell. Eu^{2+} would be an unusual oxidation state in zircon and, to our knowledge, no detailed EPR study has been carried out. Vinokurov et al. (1963b) have, however, reported detecting small amounts of Eu^{2+} (along with Gd^{3+}, Nb^{4+}) by EPR. Krasnobaev et al. (KVK88, p. 82) report detailed K-band EPR results, including hfs from ^{151}Eu ($I = 5/2$, 47.1%) and ^{153}Eu ($I = 5/2$, 52.9%), for Eu^{2+} in xenotime, (see also Kurbanov et al. 1981).

Gd^{3+} is one of a group of three lanthanides (others, Eu^{2+}, Tb^{4+}) with half-filled $4f$ shells for which, in principle, EPR is relatively simple. With ground state $^8S_{7/2}$ the $4f^7$ ions are expected to have reasonably isotropic g parameter matrices and relatively small zfs. Gd^{3+} has been relatively well studied by EPR in tetragonal crystals of the zircon (Abraham et al. 1969; Reynolds et al. 1972) and scheelite (Meil'man 1967; Vinokurov and Stepanov 1967) structures. Dudar et al. (1984) determined the relative concentrations of the paramagnetic centres Gd^{3+}, Tb^{4+}, Nb^{4+} (and Ti^{3+}) from combined EPR and optical studies of zircons. The first reported EPR SH analyses of Gd^{3+} in zircon are the X- and Q-band measurements of Hutton and Troup (1964). They studied a natural single crystal at 77 and 290 K. The analysis and magnitudes of parameters reported are similar to, but less precise than, those reported by Abraham et al. (1969); these are given in more detail below. Hutton and Troup (1969) also reported isotropic hyperfine interaction constants from the two isotopes ^{155}Gd ($I = 3/2$, 14.8%) and ^{157}Gd ($I = 3/2$, 15.7%) the values being 3.47(1) and 4.53(1),

respectively; the ratio 0.766(4) is in good agreement with that of the nuclear g factors for the two isotopes, namely 0.764 (Weil and Rao 1995). Abraham et al. (1969) reported X-band EPR studies of Gd^{3+} in the isomorphous crystals zircon, hafnon and thorium silicate, $ThSiO_4$, over the temperature range 1.2 – 300 K. Uniaxial spectra were observed in each case indicating D_{2d} symmetry and substitution of Gd for Zr, Hf or Th. The results were fitted to an SH appropriate to a site of Laue class $4/mmm$ containing an electronic Zeeman term and zfs terms, expressed in the Stevens notation, namely

$$\mathscr{H}_{zfs} = B_2^0 O_2^0 + B_4^0 O_4^0 + B_4^4 O_4^4 + B_6^0 O_6^0 + B_6^4 O_6^4 .$$

The parameters determined from the 300-K measurements were for $Gd^{3+}/ZrSiO_4$: $g_\parallel = 1.9917(5)$, $g_\perp = 1.9912(10)$, $D = b_2^0 = 3B_2^0 = -377.2(1)$ G, $b_4^0 = 60B_4^0 = 8.13(3)$ G, $b_4^4 = 60B_4^4 = 68.7(7)$ G, $b_6^0 = 1260B_6^0 = 0.65(3)$, $b_6^4 = 1260B_6^4 = 1(1)$. Only the parameter b_2^0 varied significantly in the temperature range 1.2 – 300 K. The sign of b_2^0 ($= D$) was determined by depopulation experiments between 1.2 and 4.2 K; the signs of the other parameters are known relative to b_2^0. Walsby (1999) re-measured a Gd^{3+} spectrum in a natural zircon crystal using X-band EPR at ca. 15 K. The results for angular-dependent data in the crystal bc plane were fitted to the same SH as used by Hutton and Troup (1964) and Abraham et al. (1969), but expressed in tesseral combinations of spherical tensor operators and including extra high-spin terms of dimension BS^3, BS^5. The analysis was by full matrix least squares (Mombourquette et al. 1996). Within error, the parameter magnitudes agreed with those of Abraham et al. (1969) and only high-spin terms of dimension BS^3 were found to be statistically significant. The nature of luminescence and capture centres in zircon crystals containing Gd^{3+} has been discussed by Lysakov et al. (1976).

EPR of Tb^{4+} in natural and synthetic zircons has been the subject of papers by Hutton and Milne (1969), Bershov (1971) and later Hansen et al. (1996). The first-named authors used both X and Q band EPR measurements at room temperature. Hansen et al. also utilised X and Q band EPR and made measurements at three temperatures, 50, 77 and 293 K. Hutton and Milne (1969) assumed an isotropic g [given as 2.003(1)] while Hansen et al. give $g_\parallel = 1.999(2)$ and $g_\perp = 1.989(2)$; the deviation from isotropy is, however, small. The second-degree fine-structure parameter, b_2^0, on the other hand, differs considerably in the two works: Hutton and Milne give $b_2^0 = \pm 823(3)$ kG while Hansen et al. quote $b_2^0 = 903.9(5)$ kG. (The sign of b_2^0 as well as the signs of fourth-degree zfs parameters were obtained by "comparing the intensity of certain transitions at various temperatures"). The magnitude of the zfs is very large and is said by Hutton and Milne (1969) to be "the largest yet reported" for an S-state ion.

It is convenient to discuss EPR of Er^{3+} and Dy^{3+} in zircon, and zircon-type crystals, together. Dy^{3+} has a $4f^9$ electronic configuration and Er^{3+} a $4f^{11}$ configuration. The free ion ground state is $^4I_{15/2}$ for the former and $^4H_{15/2}$ for the latter (Abragam and Bleaney 1969). In each case, the $J = 15/2$ level will be split into eight Kramers' doublets in crystal fields of tetragonal or lower symmetry and the zfs are expected to be such that only the lowest doublet will be appreciably populated, at least at low temperatures. Ball (1971) reported EPR results for both ions in natural single crystals of zircon using both X- and Q-band measurements at 4.2 K. The spectra were uniaxial in both cases. For Dy^{3+} the EPR parameters for the lowest doublet with effective spin 1/2 were given as: $g_{||} = 1.132(1)$, $g_{\perp} = 9.974(2)$. Hfs due to two isotopes ^{161}Dy ($I = 5/2$, 19.0%) and ^{163}Dy ($I = 5/2$, 2.49%) identified the centre unambiguously and gave: $A_{||} = 33(1)$ G, $A_{\perp} = 301(1)$ G for the former and $A_{||} = 43(1)$ G, $A_{\perp} = 425(1)$ G for the latter. Ball (1976) also studied EPR of the same two ions in the isomorphous crystal hafnon.

EPR of Er^{3+} in zircon has been the subject of papers by Valishev et al. (1965), Ball (1971) and Reynolds et al. (1972); Ball (1976) also studied Er^{3+} in hafnon and Reynolds et al. (1972) studied the same ion in hafnon and thorium silicate. In zircon, Ball (1971) gives the following parameters for the axially symmetric Er^{3+} spectrum of the effective spin $S = 1/2$ ground doublet observed at 4.2 K using both X- and Q-band instruments: $g_{||} = 3.703(1)$, $g_{\perp} = 6.971(2)$, $A_{||} = 139.07(5)$ G, $A_{\perp} = 263.9(1)$ G, $P_{||} = 14.98(1)$ G. The earlier results of Valishev et al. (1965) are in reasonable agreement. Reynolds et al. (1972) observed two spectra at 4.2 K attributed to Er^{3+}. The first was an axially symmetric spectrum for which parameters were obtained in fairly good agreement with those of Ball (1971) above. The second spectrum is described as an "orthorhombic" spectrum, that is, a spectrum giving three distinct g values. The site splittings observed identify the spectrum as arising from an ion in a site of Laue class $2/m$ (i.e. point-group symmetry m, 2, $2/m$) with one of the principal g (g_{yy}) values for the effective spin $S = 1/2$ lying along one of the dihedral two fold axes of the zircon unit cell, $2/m^3$ in the nomenclature of Rae (1969). Reference to the unit cell of zircon shows that the point-group symmetry of the site of the Er^{3+} ion must be 2 (C_2). The other two principal directions lie in the $(1\ 1\ 0)$ plane, making angles 38° and 52° with c. The g values given are: $g_{xx} = 0.31(3)$, $g_{yy} = 15.08(2)$, $g_{zz} = 2.145$.

Reynolds et al. (1972) also reported EPR measurements on Yb^{3+} in zircon-structure silicates, zirconium, hafnium and thorium silicate, while Ball (1982) reported EPR studies on Yb^{3+} (and Nd^{3+}) in zircon and hafnon. The free-ion configuration and ground state of Yb^{3+} are $4f^{13}$ and $^2F_{7/2}$, respectively. A tetragonal field will split the ground term into four Kramers' doublets and paramagnetic resonance is expected in the lowest doublet with effective spin $S = 1/2$. Reynolds et al. (1972) did not observe an axially symmetric spectrum of Yb^{3+}

but reported again an "orthorhombic" spectrum, which as for Er^{3+} above arises from an ion in a site of $2/m$ Laue class. Again g_{yy}, in the axis choice of the authors, lies along $[1\ 1\ 0]$ establishing the point-group symmetry of the site as 2 (C_2). The reported g values are: $g_{xx} = 2.782(2)$, $g_{yy} = 2.530(2)$, $g_{zz} = 3.292(2)$. No hyperfine structure was reported. Ball (1982) studied an axially symmetric spectrum in zircon attributed to Yb^{3+} at 15 K. Reported parameters, including hfs parameters, for the two Yb isotopes ^{171}Yb ($I = 1/2$, 14.3%) and ^{173}Yb ($I = 5/2$, 16.6%) are as follows: $g_{||} = 6.9537(5)$, $g_{\perp} = 0.435(1)$, ^{171}Yb $A_{||} = 1967(1)$ G, $A_{\perp} = 541.9(2)$ G, ^{173}Yb $A_{||} = 118(53)$ G, $A_{\perp} = 21(10)$ G. Assuming an isolated ground-state wavefunction of the form $a|\pm 9/2\rangle + b|\pm 1/2\rangle + c|\mp 7/2\rangle$, Ball calculated $g_{||} = 6.954$, $g_{\perp} = 1.94$, the latter being in poor agreement with experiment. Considerable mixing of excited spin states was therefore inferred.

Actinide ions

So far as we are aware, Np^{4+} is the only actinide ion to have been studied by EPR in zircon. Other ions and oxidation states of interest might be Th^{3+} ($5f^1$), U^{3+} ($5f^3$) and Cm^{3+} ($5f^7$). Thorium silicate is isomorphous with zircon and one might expect to observe a Th^{3+} centre analogous to the Zr^{3+} centre formed in irradiated zircon, but no such centre seems to have been observed. Fielding (1970) reported colour centres in zircon containing both Eu^{3+} and U^{4+} ions, but no EPR studies were reported. Abraham et al. (1969) reported attempted EPR measurements on Cm^{3+}-containing crystals of zircon, hafnon and thorium silicate at temperatures down to 1.2 K. No spectra were observed and this was attributed to the expected very large zfs of the Cm^{3+} ion. Poirot et al. (1988) reported optical and EPR studies of Np^{4+}-doped zircon crystals. The concentration of Np in the crystal was determined by γ-ray counting methods according to the known decay path of the radioactive $^{237}_{93}Np$ nuclide; ^{237}Np has a nuclear spin $I = 5/2$. The EPR measurements were carried out at 4.2 K using a 35-GHz, Q-band instrument. The reported SH parameters from observation of resonances in the lowest-lying $S_{eff} = 1/2$ doublet for an ion in a site of point-group symmetry D_{2d} are: $|g_{||}| = 0.8(6)$, $|g_{\perp}| = 2.59(2)$, $A_{||} = -856(428)$ G, $A_{\perp} = 1695(11)$ G. Together, the optical and EPR data indicated a ground state corresponding to $J = 9/2$ and negligible admixture with excited spin states.

Miscellaneous electron centres

We report here a few electron centres that do not fit easily into one of the preceding sections. They are of two types: (1) radical clusters which appear to have trapped an electron to form a paramagnetic species and (2) centres, which from the g values are evidently electron-trap

transition ion centres, but the transition ion is not (cannot be) identified. Solntsev et al. (1974) reported three radical ion centres of the first type, namely SiO_2^-, SiO_3^{3-}, SiO_4^{5-}, for each of which the measured g values were less than or equal to the free-electron value. Furthermore, the identities of the species were inferred by comparing the principal g and A values and their directions to known iso-electronic species for which EPR data is available, e.g. SiO_2^- with CO_2^- each of which 17 valence electrons. It is noted that no hfs was reported for any of these centres.

Lees (2001) has reported two centres in a synthetic crystal deliberately doped with varying amounts of boron in an attempt to duplicate, and perhaps find variants of, a $[BO_4]^0$-hole centre (discussed later) formed by X-irradiation of a nominally pure synthetic zircon crystal at 77 K. In addition to the said hole centre, two further centres were found. The first exhibited (super) hfs from a single B and, from the observed site splittings in the planes of measurement, originated from a site of Laue class mmm orthorhombic ($mm2$ point-group symmetry from the available sites in zircon). The principal values: g matrix: 1.968755(5), 1.98092(1), 1.96859(1) and [11]B, A matrix: 0.638(8) G, 0.17(2) G, 0.19(2) G were found. The second centre exhibited (super) hfs from two B atoms. The site splitting indicated a site of Laue class $2/m$ (point-group symmetry m). The principal values for the two boron centre: g matrix: 1.982145(9), 1.96936(1), 1.969251(8) and [11]B, A matrix: 4.99(2) G, 4.34(2) G, 4.16(1) G were reported. The magnitude and anisotropy of the g values indicate an electron trapped on a transition metal ion, but there was no observed hfs to identify the ion. Furthermore, the small magnitudes of the observed [11]B-hyperfine splittings precluded an elec-

tron centre with the electron trapped at B. The presence of B was established unambiguously in the case of the second centre by fitting hfs from the second less abundant [10]B ($I = 3$, 19.8%) isotope in some crystal orientations. The ratio of fitted hyperfine splittings reflected accurately those expected from the ratio of the respective nuclear g values. The identity of the proposed electron centres is not known at this stage. It should be emphasised that the site symmetry of the first centre is seen from the observed site splittings to be $mm2$. Other reported orthorhombic species in zircon are frequently those for which the g parameter matrix is orthorhombic (i.e. has three distinct principal values), which is necessarily so for any site of lower than uniaxial symmetry.

Electron-deficient centres

Electron-deficient centres in zircon are almost invariably, those, where an electron has been removed from a ligand-oxygen as a result of ionising irradiation. They are characterised by g values that usually exceed the free electron value. Considering that there is but one type of O atom in the zircon lattice, EPR studies of oxygenic-hole centres form a surprisingly complex field. This is well illustrated from the examples in the review article by Krasnobaev et al. (KVK88, pp. 88–96).

Figure 4, adapted and expanded from Fig. 55 of Krasnobaev et al. (KVK88, p. 90), illustrates the range of g values, from almost isotropic to highly anisotropic, obtained for 30 reasonably well-characterised oxygenic-hole centres. The corresponding orbital splittings, obtained (see Claridge et al. 2000a) from a crystal-field

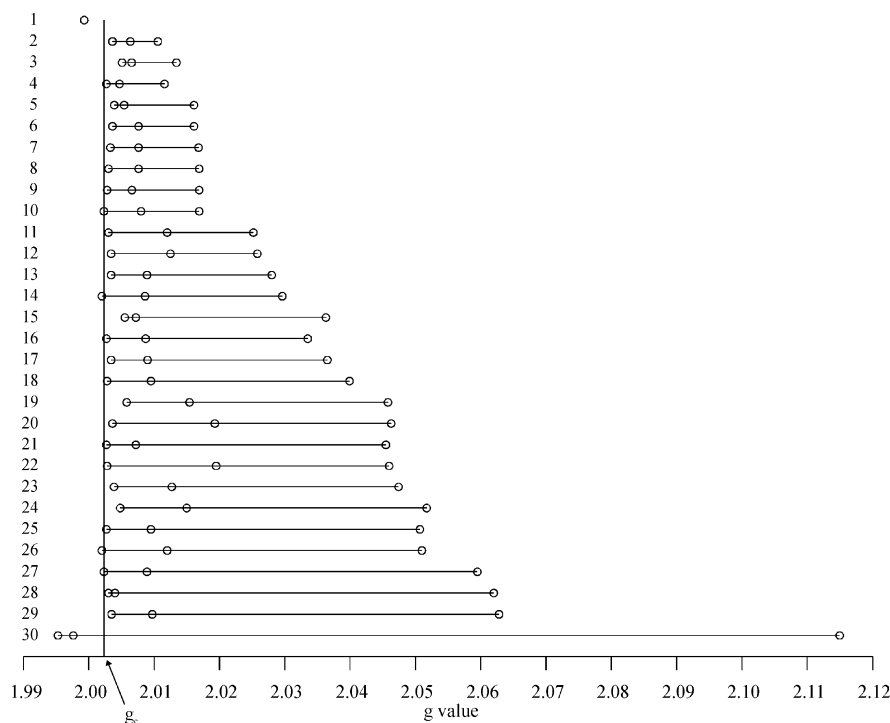**Fig. 4** Depiction of g values for some hole centres observed by EPR in zircon

Table 1 Listing of designations and references to the hole centres depicted in Fig. 4

Sample no. (Fig. 4)	Brief description/ designation	Reference
1	$SiO_4^{3-}/Vac(Zr)$ (C centre)	Claridge et al. (1999b)
2	SiO_4^{3-} (D centre)	Claridge et al. (1994a)
3	SiO_4^{3-} (RTcentre)	Claridge et al. (1994a)
4	SiO_2^{3-}	Krasnobaev et al. (1988)
5	SiO_2^{3-}/OH^-	Krasnobaev et al. (1988)
6	SiO_4^{3-}/Y^{3+}	Barker and Hutton (1973)
7	SiO_4^{3-}/Y^{3+}	Vinokurov et al. (1971)
8	$SiO_2^{3-}/2Y^{3+}$	Krasnobaev et al. (1988)
9	SiO_2^{3-}/Y^{3+}	Krasnobaev et al. (1988)
10	$[SiO_3 - SiO_4]^{5-} - Y^{3+}$	Solntsev and Shcherbakova (1973a)
11	SiO_4^{3-}/Y^{3+} (290 K)	Danby and Hutton (1980)
12	SiO_3^-/Y^{3+}	Krasnobaev et al. (1988)
13	AlO_3^{2-}	Krasnobaev et al. (1988)
14	SiO_4^{3-}/Y^{3+} (77 K)	Danby and Hutton (1980)
15	SiO_3^-/H^+	Krasnobaev et al. (1988)
16	$SiO_3^-/2H^+$	Krasnobaev et al. (1988)
17	$SiO_3^-/Vac(Zr)$	Krasnobaev et al. (1988)
18	SiO_4^{3-}/OH^-	Krasnobaev et al. (1988)
19	AsO_4^{2-} (see text)	Krasnobaev et al. (1988)
20	$SiO_4^{3-}/2H^+$	Krasnobaev et al. (1988)
21	$SiO_3^-/[H_2O + Vac(Zr)]$	Krasnobaev et al. (1988)
22	$SiO_4^{3-}/[H_2O + Vac(Zr) + Vac(O)]$	Krasnobaev et al. (1988)
23	$[BO_4]^0$	Walsby et al. (2000)
24	$[AlO_4]^0$	Claridge et al. (1994b)
25	AlO_4^{4-}	Krasnobaev et al. (1988)
26	AlO_4^{4-}	Solntsev and Shcherbakova (1973a)
27	SiO_4^{3-}/Y^{3+}	Krasnobaev et al. (1988)
28	SiO_4^{3-}	Solntsev and Shcherboakova (1973a)
29	$[SiO_4/Y]^0$	Claridge et al. (2000a)
30	$[SiO_4/M]^0$	Claridge et al. (2000a)

analysis of the principal *g* values, cover a range from a few thousand cm^{-1} to almost complete orbital quenching (see Claridge et al. 1999b). Brief descriptions or designations of the hole centres of Fig. 4 together with references are listed Table 1.

The nomenclatures used for describing electron-deficient centres need to be considered briefly. Most of the centres studied have been described in terms of an SiO_4^{3-} unit whereby an electron has been removed from the *p* orbital of a ligand oxygen leaving a trapped hole in a *p* orbital of an O$^-$-ion. The hole will become "trapped" only if the O in question differs from other nearby oxygens, since otherwise there is nothing to stop the hole from wandering, and generally no EPR spectrum would be expected. For discussions on this point see Gainullina et al. (1971) and Claridge et al. (2000a). Also electrical balance demands that the reduced negative charge on the unit containing the hole be balanced by a cation substituting for Si or Zr with charge (usually) one less than $+4$, that of Zr and Si in the lattice. These considerations lead to the designation, $[SiO_4^{3-}/M^{3+}]^0$ (or simply $[SiO_4/M]^0$) (Claridge et al. 2000a), where in this case the hole is stabilised (trapped) by a $+3$ cation which may substitute in either of the Zr or Si lattice positions (see also Weil 1984 for discussion of similar designations

in α-quartz). In the case of M substituting for Si in the lattice, the centre may be designated simply $[MO_4]^0$ where M is a $+3$ cation such as Al or B. The nomenclature of Claridge et al. differs from that of Krasnobaev et al. and others, who refer to the true charge of the cluster rather than the departure of the cluster from the unperturbed state. Thus, for example, AlO_4^{4-} and $[AlO_4]^0$ are equivalent. Other electron-deficient centres, said to contain units such as SiO_3^-, SiO_2^-, SiO_2^{3-} (Solntsev et al. 1974; see also KVK88, pp. 88–96) with appropriate associated stabilising ions, have been reported. In these cases, for units located in lattice positions, removal of one or more oxygens is required. In such a case one would presumably have the possibility of formation of F-type centres whereby an electron becomes trapped at an anion vacancy. So far as we are aware, no F-centre paramagnetic species have been reported from EPR studies on zircons. There is also the possibility, albeit remote because of space restrictions, of oxygen-deficient units existing as radicals in some interstitial position in the lattice, but we are not aware of any reports of such centres in zircon. In the section that follows we shall be content to refer, wherever possible, to the data of Fig. 4 rather than quote principal *g* values for the hole centres under discussion.

Solntsev and Shcherbakova (1973a) reported a hole centre designated SiO_4^{3-} (Fig. 4, no. 28) and a second, observed in a high Y-containing crystal designated [SiO_3-SiO_4]$^{5-}$/2Y^{3+} (Fig. 4, no. 10) in which hfs from two equivalent ^{89}Y nuclei was observed. These authors also reported a centre designated AlO_4^{4-} where hfs from ^{27}Al was also reported. This centre is analogous to the [AlO_4]^0 centre observed in α-quartz (see Nuttall and Weil 1981, and references therein to earlier papers). As described below, other authors have also reported the same centre.

Barker and Hutton (1973) reported a hole centre [SiO_4/Y]^0 (Fig. 4, no. 6), which from the observed site splitting, indicated a site of only $\bar{1}$ Laue class. This is the same centre previously reported by Matumura and Koga (1962, 1963), who wrongly attributed the centre to a triplet species, and Vinokurov et al. (1971) (Fig. 4, no. 7), who proposed a hole centre model based on O$^-$ interacting with ^{89}Y). From the g and ^{89}Y A principal directions, Barker and Hutton (1973) propose that the centre is a hole situated on O and stabilised by Y substituting for Zr where the O is "long-bonded". However, the symmetry would then be expected to be m (C_s) unless one or other of O or Y was considerably shifted from its normal lattice position. In a later paper, Danby and Hutton (1980) (Fig. 4, no. 11) reported a second hole-centre "similar to that already described" (Barker and Hutton 1973). In this second centre the symmetry, as exemplified by the site splitting, changed from m to $\bar{1}$ as the temperature was lowered from 290 to 77 K. The authors explain this in terms of motion of the Y^{3+} ion away from its coplanar site with the oxygenic hole. Below the transition temperature (230 K) thermal motion is insufficient to overcome the potential barrier between the two positions. Above the transition temperature the Y sites are motionally averaged and apparently higher symmetry is observed. This centre may be the same as that reported by Krasnobaev et al. (KVK88, p. 90, Fig. 55; Fig. 4, no. 12, this paper).

Claridge et al. (1994a) described 10-K X-band EPR studies of two previously unreported hole-centres labelled D and RT (Fig. 4, nos. 2, 3, respectively). From the observed site splitting in the bc and ab planes the symmetry of each was established as $2/m$ Laue class and thus to point-group symmetry m (C_s), the point-group symmetry of all oxygens in the lattice. Both centres are relatively easily power-saturated, requiring all measurements to be made at low microwave power (∼0.05 mW). They differ in that D is observable only at temperatures below 77 K while RT, as the designation implies, is observable at ambient temperatures. Hfs, probably due to one or more interacting ^{29}Si nuclei, was observed but was too weak for definitive angular dependence studies. Comparison of principal g matrix directions with bond directions of the ideal lattice led to the conclusion that The D centre is a hole centre trapped at a short-bonded O and RT to a hole trapped at a long-bonded O with respect to a given Zr position. Alternatively, and equivalently, they could be envisaged as being trapped on the same O with their g matrices related by a 17.6

rotation about b, the inherent two fold axis common to both (see a further note below on orientation of hole centre principal directions).

Solntsev and Shcherbakova (1973a; Fig. 4, no. 26), Krasnobaev et al. (KVK88, p. 90, Fig. 55: Fig. 4, no. 25 this paper) and Claridge et al. (1994b) (Fig. 4, no. 24) all reported results on a Al-stabilised oxygenic hole centre, which, as outlined earlier, we shall designate [AlO_4]^0. Allowing for small differences in the measured g values, it would seem probable that all three papers refer to the same centre. We shall discuss only the third of these references since it is more precise and complete than the other two. These authors (Claridge et al. 1994b) report precise interaction matrices for g, A (^{27}Al) and P (^{27}Al). As required of a site of point-group symmetry m, all three matrices have one principal value, not generally the largest-magnitude one, lying along the inherent two fold axis, i.e. along the axis perpendicular to the mirror plane containing both O and Al. The directions of the other two principal values of the three matrices are non-coaxial. One principal direction of the ^{27}Al A matrix lies almost exactly along the Al–O direction. The maximum magnitude principal value of the nuclear electric quadrupole matrix does not lie along this direction, indicating probably that the electric-field gradient is not dominated by the electron hole, as it is evidently in the equivalent hole centre in α-quartz (Nuttall and Weil 1981).

Closely related to the [AlO_4]^0 centre is a centre designated [BO_4]^0 reported recently by Walsby et al. (2000) (Fig. 4, no. 23) from 15-K X-band EPR studies. Precise g, ^{11}B ($I = 3/2$, 80.2%) A and P matrices were determined. For crystal orientations close to b it was possible to observe and measure hfs (seven lines) due to the less abundant ^{10}B isotope ($I = 3$, 19.8%). The following relationship $g_n(^{10}B)/g_n(^{11}B) = (^{10}B)/A(^{11}B)$ should apply. The ratios given by EPR and nuclear g values (Weil and Rao 2000) are 0.335 and 0.337, respectively, thus confirming the presence of B. In this case, one principal direction of both the hyperfine and nuclear electric quadrupole matrices lay, within error, along the B–O bond direction. As for the [AlO_4]^0 centre in α-quartz, the electric-field gradient is dominated by the trapped hole, stabilised in this instance by B. A crystal-field analysis of the g values using matrix diagonalisation of the crystal-field spin-orbit coupling matrix showed that the ordering and the splitting of the p orbitals of the [BO_4]^0 and [AlO_4]^0 are similar. The centre, no. 19, designated AsO_4^{2-} in Table 1, produces g values which are very close to those given by Walsby et al. (2000) for [BO_4]^0 and may be the same centre. It is noted that the super hfs from either ^{11}B ($I = 3/2$, 80.2%) or ^{75}As ($I = 3/2$, 100%) could easily be misdiagnosed.

Claridge et al. (1997b) reported an "unusual" centre in zircon that, as discussed in the 1st-row transition centres, turned out (Claridge et al. 1999b) to be two distinct centres, one a Cr^{3+}/Si centre (discussed earlier) and the other a hole centre. We now report this latter centre, designated C (Fig. 4, no. 1) in the two papers of

the previous sentence, and its interpretation. From Fig. 4 the C centre is seen to be unique amongst the hole centres listed: its g values are almost isotropic [1.99939(1), 1.99937(1), 1.99924(1)] and are less than the free-electron value. The centre was formed by X-irradiation of a nominally pure zircon crystal at 77 K followed by cold transfer to the EPR cavity; subsequent annealing of the crystal to room temperature left the centre unchanged. Claridge et al. (1999b) proposed that the centre is an oxygenic-hole centre where the oxygen $2p$ hole orbital is oriented towards a nearest-neighbour Zr^{4+} vacancy that stabilises the hole by Coulomb forces, thus explaining the high thermal stability of the centre. Hyperfine interactions with one ^{29}Si and one ^{91}Zr neighbour were explained including exchange polarisation effects and the near isotropic g values by near complete orbital quenching. Krasnobaev et al. (KVK88, nos. 9, 12, 13 of their Fig. 55) reported three centres that were proposed to involve Zr^{4+} vacancies. However, each of these centres has anisotropic g values in the range 2.003–2.045.

Claridge et al. (2000a) reported two further hole centres designated $[SiO_4/Y]^0$ and $[SiO_4/M]^0$, where the first exhibits hfs from ^{89}Y and the second a cation of +ve valence less than the +4 of Zr (or Si) was inferred. If lower than +3, the second centre would, of course, be charged and require a remote compensator for charge balance. The two new centres are nos. 29 and 30 of Fig. 4. The second of the centres has, so far as we are aware, the most anisotropic g values of any reported zircon hole centre; also two g values are less than the free-electron value. In this paper Claridge et al. (2000a) attempted also to systematise the structure of the hole centres in zircon and to account for the plethora of centres observed. The model was that utilised earlier to describe similar centres in α-SiO_2 (Griffiths et al. 1954; Nuttall and Weil 1981), GeO_2 (Stapelbroek et al. 1976, 1977) and β-Al_2O_3 (Barklie et al. 1983). The hole is thought to be trapped in a p-orbital, normally the p_z orbital according to a crystal-field analysis, of an O^- ion (leaving an electron with unpaired spin in this orbital) and stabilised by an impurity cation located in one of the Zr or Si lattice positions. The crystal-field analysis followed that of Vannotti and Morton (1968) for an S^- hole and Stapelbroek et al. (1976) for O^- except that numerical diagonalisations of the energy matrices involved were utilised. The cation evidently enhances the stability of the centre if it is of lower positive valence than that of Zr^{4+}; Al^{3+} (Claridge et al. 1994b), B^{3+} (Walsby et al. 2000) and Y^{3+} (Claridge et al. 2000a and references therein) are examples of +3 cations which have been identified via their signature hfs in each case. A more extreme example of this mechanism is that of the C centre reported above where the oxygenic hole is stabilised by an adjacent Zr^{4+} vacancy; in this case the centre is particularly stable, i.e. the hole can be said to be in a very "deep" trap. Similarly, the so-called RT centre (Claridge et al. 1994a) is evidently particularly stable, and in this case a +2 ion, perhaps Ca^{2+}, for which no

hfs would be observable, has been suggested (Claridge et al. 2000a). The centre $[SiO_4/M]^0$ (Fig. 4, no. 30) is also a centre not completely understood. Claridge et al. (2000a) suggested a p_x ground-state orbital for the trapped hole, as distinct from p_z in general, but further work by Lees (2001) has shown that it is not necessary to invoke a p_x orbital to effect a crystal-field analysis of the g values.

It remains to report and comment briefly on some oxygen-deficient hole centres that have been reported from EPR studies on zircon. Krasnobaev et al. (KVK88, p. 90, Fig. 55) report a number of centres of the type $\left[SiO_2^{3-}/X\right]$ and $\left[SiO_3^-/X\right]$ where $X =$ one of Y^{3+}, $2Y^{3+}$, H^+, $2H^+$, OH^- together sometimes with a Zr^{4+} vacancy. Gramolin et al. (1982), from whom some of the above was taken, reported EPR of $\left[SiO_2^{3-}\right]$ and $\left[SiO_3^-\right]$ silicate complexes stabilised by Y^{3+} ions in natural zircons. In order to establish unambiguously the presence of O vacancies in such centres it will be necessary to carry out at the least very precise angular-dependent measurements together with matrix diagonalisation of the resulting SH to obtain precise directional information on the various parameter matrices. We note that in several instances, from the reported g values, some centres with alternative designations may well be the same centre (see and compare for example nos. 2–10 in Fig 3). In addition, one should look for evidence of F-centre type centres that would be expected if there are anion vacancies in the lattice.

References

Abragam A, Bleaney B (1970) Electron paramagnetic resonance of transition ions. Clarendon, Oxford

Abragam A, Pryce MLH (1951) Theory of nuclear hyperfine structure of paramagnetic resonance spectra in crystals. Proc Roy Soc (London) (A) 205:135–153

Abraham MM, Clark GW, Finch CB, Reynolds RW, Zeldes H (1969) Ground-state splitting of trivalent Gd and Cm in $ZrSiO_4$, $HfSiO_4$, and $ThSiO_4$, determined by ESR. J Chem Phys 50:2057–2062

Abraham MM, Boatner LA, Ramey JO, Rappaz M (1984) The occurrence and stability of zirconium in orthophosphate single crystals. J Chem Phys 81:5362–5366

Bailey P, Weil JA (1992) EPR of $[TiO_4/Li]^0_\beta$ and related centers in X-irradiated α-quartz. J Phys Chem Solids 53:601–610

Ball D (1971) Paramagnetic resonance of Er^{3+} and Dy^{3+} in natural single crystals of zircon. Phys Status Solidi (B) 46:635–641

Ball D (1976) Paramagnetic resonance of Er^{3+} and Dy^{3+} in synthetic single crystals of hafnon. Phys Status Solidi (A) 35:651–658

Ball D (1982) The paramagnetic resonance of Nd^{3+} and Yb^{3+} in zircon structure silicates. Phys Status Solidi (B) 111:311–320

Ball D, Lowther JE (1977) Jahn–Teller effects and hyperfine parameters of V^{4+} on tetragonally distorted tetrahedral sites. Phys Lett (A) 61:333–335

Ball D, Van Wyk JA (2000) The electron paramagnetic resonance of Fe^{3+} observed in two axial sites in synthetic single crystals of zircon ($ZrSiO_4$). Phys Status Solidi (B) 218:545–551

Ball D, Wanklyn BM (1976) Coloured synthetic zircon crystals. Phys Status Solidi (A) 36:307–316

Ballman AA, Laudise RA (1965) Crystallization and solubility of zircon and phenacite in certain molten salts. J Am Ceram Soc 48:130–133

Barker PR, Hutton DR (1973) A colour centre in natural zircon. Phys Status Solidi (B) 60:K109-K111

Barklie RC, Niklas JR, Spaeth J-M, Bartram RH (1983) ENDOR and EPR of defects in relatively stoichiometric β-alumina. J Phys (C) Solid State Phys 16:579–590

Belletti A, Borromei R, Oleari L (1995) Absorption spectra of zircon crystals doped with Cr(IV): $ZrSiO_4$: Cr^{4+}. Inorg Chim Acta 235:349–355

Beltrán A, Bohm S, Flores-Riveros A, Igualada JA, Monrós G, Andrés J, Luaña V, Pendás M (1993) Ab initio cluster-in-the-lattice description of vanadium-doped zircon. Analysis of the impurity centers V^{4+}: $ZrSiO_4$. J Phys Chem 97:2555–2559

Bershov LV (1971) Isomorphism of terbium (IV), thulium (II) and yttrium (III) in zircons. Geokhimiya 1:48–53

Binks W (1926) The crystalline structure of zircon. Mineral Mag 21:176–187

Buckmaster HA, Chatterjee R, Shing YH (1972) The application of tensor operators in the analysis of EPR and ENDOR spectra. Phys Status Solidi (A) 13:9–50

Buckmaster HA, Chatterjee R (1998) The analysis of EPR spectra using tesseral tensor angular momentum operators. Phys Status Solidi (B) 209:433–441

Chase AB, Osmer JA (1966) Growth and preferential doping of zircon and thorite. J Electrochem Soc 113:198–199

Claridge RFC, Mackle KM, Sutton GLA, Tennant WC (1994a) Zircon EPR revisited: 10-K EPR of three low-symmetry centres in irradiated zircon (zircon silicate). J Phys Condens Matter 6:3429–3436

Claridge RFC, Mackle KM, Sutton GLA, Tennant WC (1994b) 10-K EPR of an oxygen-hole aluminium centre, $[AlO_4]^0$, in X-irradiated zircon, $ZrSiO_4$. J Phys Condens Matter 6:10415–10422

Claridge RFC, McGavin DG, Tennant WC (1995) 10-K electron paramagnetic resonance of a d^1 Ti^{3+} centre in X-irradiated zircon (zirconium silicate), J Phys Condens Matter 7:9049–9060

Claridge RFC, Tennant WC (1997) Recent 10-K EPR studies of radiation induced defects in zircon. In: Rudowicz CZ (ed) Modern Applications of EPR/ESR: Proc of 1st Asia-Pacific EPR/ESR Symposium, Hong kong, pp 465–472

Claridge RFC, Taylor KC, Tennant WC, Walsby CJ (1997a) X-band electron paramagnetic resonance of a new Ti^{3+} centre in X-irradiated zircon. J Phys Condens Matter 9:3075–3080

Claridge RFC, Sutton GLA, Tennant WC (1997b) X-band EPR study of an unusual center in X-irradiated zircon at 10 K. J Magn Reson 125:107–113

Claridge RFC, Lees NS, Tennant WC, Walsby CJ (1999a) Two Ti^{3+} centres studied by X-band electron paramagnetic resonance at 10 K in zircon. J Phys Condens Matter 11:3571–3580

Claridge RFC, Tennant WC, Schweizer S, Spaeth J-M (1999b) Structural models for room-temperature stable radiation-induced centres in zircon. J Phys Condens Matter 11:8579–8589

Claridge RFC, Lees NS, Tennant WC, Walsby CJ (2000a) Oxygenic-hole centres in X-irradiated zircon: 10 K EPR studies. J Phys Condens Matter 12:1431–1440

Claridge RFC, Tennant WC, Walsby CJ, Schweizer S, Spaeth J-M (2000b) An EPR/ENDOR investigation of a $[ZrPO_4]^0$ centre in X-irradiated zircon: the Zr(α) centre. J Phys Condens Matter 12:1421–1430

Danby RJ, Hutton DR (1980) A new radiation centre in natural zircon. Phys Status Solidi (B) 98:K125-K128

Dharmarajan R, Belt RF, Puttbach RC (1972) Hydrothermal and flux growth of zircon crystals. J Crystal Growth 13/14:535–539

Di Gregorio S, Greenblatt M, Pifer JH (1980) ESR of Nb^{4+} in zircon. Phys Status Solidi (B) 101:K147–K150

Di Gregorio S, Greenblatt M, Pifer JH, Sturge MD (1982) An ESR and optical study of V^{4+} in zircon-type crystals. J Chem Phys 76:2931–2937

Dudar LP, Votyakov SL, Gramolin AB, Krasnobaev AA, Krokhalev VYa, Fishman MV (1984) Spectroscopic properties of zircons from kimberlite rocks of Timan. Tr-Akad Nauk SSSR, Komi Fil, Inst Geol 46:84–89

Dziesiaty J, Peka P, Lehr MU, Schulz H-J, Klimakow A (1994) Electron paramagnetic resonance related to optical charge-transfer processes in ZnSe: Ti. Phys Rev (B) 49:17011–17021

Eftaxias K, Fielding PE, Lehmann G (1989) Mo^{5+} in synthetic zircon crystals. Chem Phys Lett 160:36–38

Elliot RJ, Stevens KWH (1952) The theory of magnetic properties of rare earth salts: cerium ethyl sulphate. Proc Roy Soc (London) (A)215:437–453

Fielding PE (1969) Site symmetry of Eu^{3+} in flux-grown zircon. Aust J Chem 22:2463–2465

Fielding PE (1970) Colour centres in zircon containing both Eu^{3+} and U^{4+} ions. Aust J Chem 23:1513–1521

Frondel C, Collette RL (1957) Hydrothermal synthesis of zircon, thorite and huttonite. Am Mineral 42:759–765

Gaft M, Boulon G, Panczer G, Guyot Y, Reisfeld R, Votyakov S, Bulka G (2000) Unexpected luminescence of Cr^{5+} and Cr^{3+} ions in $ZrSiO_4$ zircon crystals. J Lumin 87–89:1118–1121

Gainullina NM, Efgrafova LA, Nizamutdinov NM, Vinokurov VM (1971) EPR of electron-hole centres in zircon crystals. Fiz Miner No. 3:3–13

Goldschmidt VM (1954) Geochemistry. Clarendon, Oxford

Gorz H (1974) Microprobe studies of inclusions in zircons and compilation of minor and trace elements in zircons from the literature. Chem Erde 33:326–357

Grachëv VG (1987) Correct expression for the generalized spin Hamiltonian for a noncubic paramagnetic centre. Sov Phys – JETP 65:1029–1035

Gramolin AB (1981) Paramagnetic Zr^{3+} and Hf^{3+} complexes in natural and synthetic zircons according to EPR data. Kristallokhim Osob Silik Miner Urala, Sverdlovs, pp 41–44

Gramolin AB, Votyakov SL, Krasnobaev AA (1982) EPR of SiO_2^{3-} and SiO_3^- silicate complexes stabilised by Y^{3+} ions in natural zircons. Ezhegodnik, 1981 Inf. Materialy In-t Geol i Geokhimii Ural Nauch Tsentr. AN SSSR Sverdlovsk, pp 137–140

Greenblatt M, Pifer JH, McGarvey BR, Wanklyn BM (1981) Electron spin resonance of Cr^{5+} in YPO_4 and YVO_4. J Chem Phys 74:6014–6017

Griffiths JHE, Owen J, Ward IM (1954) Paramagnetic resonance in neutron-irradiated diamond and smoky quartz. Nature 173:439–442

Hansen S, Mosel BD, Müller-Warmuth W, Fielding PE (1996) EPR studies of Tb^{4+} in single crystals of zircon and scheelite structure silicates and germanates. Z Naturforsch 51a:885–894

Harris EA, Mellor JH, Parke S (1984) Electron paramagnetic resonance of tetravalent praseodymium in zircon. Phys Status Solidi (B) 757–760

Hassel O (1926) Die Kristallstruktur einiger Verbindung von der Zusammensetzung MRO_4-I. Zirkon $ZrSiO_4$. Z Kristallogr 63:247–254

Hautefeuille P, Perrey A (1888) Synthesis of emerald and of phenacite. Compt Rend 106:1800

Hazen RM, Finger LW (1979) Crystal structure and compressibility of zircon at high pressure. Am Mineral 64:196–201

Heaman LM, Bowins R, Crocket J (1990) The chemical composition of igneous zircon suites: Implications for geochemical tracer studies. Geochim Cosmochim Acta 54:1597–1607

Henry NFM, Lonsdale K (eds) (1969) International tables for X-ray cryotallography, Vol I, Kynoch, Eng

Hoard JL, Silverton JV (1963) Stereochemistry of discrete eight-coordination, I. Basic analysis. Inorg Chem 2:235–239

Holland HD, Gottfried D (1955) The effect of nuclear radiation on the structure of zircon. Acta Crystallogr 8:291–300

Hutton DR, Milne RJ (1969) Paramagnetic resonance of Tb^{4+} in zircon. J Phys (C) Solid State Phys Ser 2 vol 2:2297–2300

Hutton DR, Troup GJ (1964) Paramagnetic resonance of Gd^{3+} in zircon. Br J Appl Phys 15:405–406

Isoya J, Tennant WC, Weil JA (1988) EPR of the TiO_4/Li center in crystalline α-quartz. J Magn Reson 79:90–98

Kikuchi C, Mataresse LM (1960) Paramagnetic-resonance absorption of ions with spin 5/2: Mn^{++} in calcite. J Chem Phys 33:601–606

Krasnobaev AA, Votyokov SL, Krochalev VYa (1988) Spectroscopy of zircons. Properties and geological applications. Nauka, Moscow

Krstanović IR (1958) Redetermination of the oxygen parameters in zircon ($ZrSiO_4$). Acta Crystallogr 11:896–897

Krstanović IR, Djurić S, Ilić P (1968) Further X-ray study of zircon (abstr). Intern Mineral Assoc, 6th General Meet, Prague, p 85

Kumar V, Kumar R, Sen K (1980) Crystal-field analysis of zircon structure Nd^{3+}: YVO_4 and $TbPO_4$. Phys Status Solidi (B) 99:K17-K21

Kurbanov KhM, Kara-Ushanov VYu, Khalikov BS (1981) Orthophosphates of rare-earth elements. Donish: Dushanbe, USSR

Laruhin MA, van Es HJ, Turkin AA, Vainshtein DI, den Hartog HW (2002) EPR study of radiation-induced defects in the thermoluminescence dating medium zircon ($ZrSiO_4$). J Phys Condens Matter 14:3813–3831

Le Page Y, Calvert LP, Gabe EJ (1980) Parameter variation in low-quartz between 94 and 298 K. J Phys Chem Solids 4:721–725

Lees NS (2001) EPR crystallography; studies of defect centres in single crystals. PhD Thesis, University of Canterbury, Christchurch, New Zealand

Lietz J (1937) Colouring of zircon by light. Naturwissenschaften 25:415–416

Lysakov VS, Solntsev VP, Eliseev AP (1976) Nature of luminescence and capture centres in zircon crystals. Zh Prikl Spektrosk 25:823–826

Marfunin AS (1974a) Isomorphous impurities and free radical formation in minerals (electron centres and hole centres). Bull Soc Fr Mineral Cristallogr 97:194–201

Marfunin AS (1974b) Introduction to the physics of minerals. Nedra: Moscow, USSR

Marfunin AS (1975) Spectroscopy, luminescence and radiation centres in minerals. Nedra: Moscow, USSR

Marfunin AS (1979) Spectroscopy, luminescence and radiation centres in minerals. Springer, Berlin Heidelberg New York

Matumura O, Koga H (1962) Colour centres in $ZrSiO_4$. J Phys Soc Jpn 17:409

Matumura O, Koga H (1963) Magnetic resonance in irradiated zircon. J Phys Soc Jpn 18: Suppl 2:312–314

McGavin DG (1987) Symmetry constraints on EPR spin-Hamiltonian parameters. J Magn Reson 74:19–55

McGavin DG, Tennant WC (1985) Coordinate rotations and relations amongst spin-Hamiltonian parameters in EPR spectroscopy. Mol Phys 55:853–866

McGavin DG, Tennant WC, Weil JA (1990) High-spin terms in the spin-Hamiltonian. J Magn Reson 87:92–109

Meil'man ML (1967) Paramagnetic resonance of gadolinium in synthetic stolzite. Sov Phys Solid State 8:2924–2925

Meil'man ML, Samoilovich MI (1977) Introduction to EPR spectroscopy of activated single crystals. Atomizdat: Moscow, USSR

Mombourquette MJ, Weil JA, McGavin DG (1996) Computer program EPRNMR. University of Saskatchewan, Canada

Nizamutdinov NM, Bulka GR, Vinokurov VM (1973) Classification of point paramagnetic defect centres in crystals based on an analysis of space groups. Sostav, Strukt Svoistva Miner 119–142

Nizamutdinov NM, Kurkin IN, Batkin AI, Vinokurov VM, Repco VP, Safronov GM, Orlovski VP, Tananaev IV (1974) EPR of neodymium (3+), erbium (3+), and dysprosium (3+) and spin-lattice relaxation of neodymium (3+) in a yttrium orthophosphate single crystal. Izv Akad Nauk SSSR, Neorg Mater 10:303–307

Nizamutdinov NM, Bulka GR, Gainullina NM, Vinokurov VM (1976) Symmetries of defect distribution in regular systems of point and the properties of the alignments of EPR spectra in crystals. In: Vinokurov VM (ed) Fiz Svoistva Miner Gorn Porod. Univ Kazan: review 45 refs)

Novak GA, Gibbs GV (1971) The crystal chemistry of the silicate garnets. Am Mineral 36:791–825

Nuttall RHD, Weil JA (1981) The magnetic properties of oxygen-hole aluminium centers in crystalline SiO_2. I. $[AlO_4]^0$. Can J Phys 59:1696–1708

Nye JF (1957) Physical properties of crystals. Their representation by matrices and tensors. Clarendon, Oxford

Poirot I, Kot W, Shalimoff G, Edelstein N, Abraham MM, Finch CB, Boatner LA (1988) Optical and EPR investigations of Np^{4+} in single crystals of $ZrSiO_4$. Phys Rev (B) 37:3255–3264

Pryce MLH (1950) A modified perturbation procedure for a problem in paramagnetism. Proc Phys Soc (A) 63:25–29

Rae AD (1969) Relationship between the experimental hamiltonian and the point group symmetry of a paramagnetic ion in a crystal. J Chem Phys 50:2672–2685

Randic M (1962) Ligand field splitting of d orbitals in eight coordinated complexes of dodecahedral structure. J Chem Phys 36:2094–2097

Reynolds RW, Boatner LA, Finch CB, Chatelain A, Abraham MM (1972) EPR investigations of Er^{3+}, Yb^{3+} and Gd^{3+} in zircon-structure silicates. J Chem Phys 56:5607–5625

Rinneberg H, Weil JA (1972) EPR studies of Ti^{3+}-H^+ centers in X-irradiated α-quartz. J Chem Phys 56:2019–2028

Robinson K, Gibbs GV, Ribbe PH (1971) The structure of zircon: a comparison with garnet. Am Mineral 56:782–790

Rudowicz C (1985) Transformation relations for the conventional O_k^q and normalised O'^q_k Stevens operator equivalents with $k = 1$ to 6 and $-k \leq q \leq k$. J Phys (C) Solid State Phys 18:1415–1430

Samatov MV, Votyakov SL (1983) Isomorphism in xenotime according to EPR data. Ezhegodnik, 1982 Inf Materialy. Int Geol i Geokhimii Ural Tsentr. AN SSSR Sverdlovsk: 106–109

Samatov MV, Votyakov SL, Krasnobaev AA (1982) Paramagnetic impurity centres in synthetic xenotime single crystals. Akad Nauk SSSR, Neorg Mater 18:1866–1868

Samatov MV, Votyakov SL, Krasnobaev AA (1983) ESR of Zr^{3+} complexes as impurities in YPO_4. Zh Strukt Khim 24:117–118

Samoilovich MI, Novozhilov AI, Barsanov GP (1968) Electron paramagnetic resonance in irradiated zircons containing various impurities. Geokhimiya 4:494–495

Solntsev VP (1973) Master's thesis. Defects in zircon and quartz detected by EPR methods. Novosibirsk, Russia

Solntsev VP (1974) Paramagnetic resonance of γ-irradiated zircons. Fiz Tverd Tela 266–273

Solntsev VP, Shcherbakova MYa (1973a) EPR study of structural defects in irradiated zircons. Dokl Akad Nauk SSSR 1:156–158

Solntsev VP, Shcherbakova MYa (1973b) Electron spin resonance of Ti^{3+} in α-quartz and zircon. Zh Strukt Khim 13:859–861

Solntsev VP, Shcherbokova MYa (1974) Mechanisms of charge compensation and form of niobium and yttrium intrusions in the zircon structure. Izv Akad Nauk SSSR, Neorg Mater 10:1834–1838

Solntsev VP, Shcherbakova MYa, Dvornikov EV (1974) SiO_2^-, SiO_3^{3-} and SiO_4^{5-} radicals in the $ZrSiO_4$ structure, from electronic paramagnetic resonance data. Zh Strukt Khim 15:217–221

Stapelbroek M, Bartram RH, Gilliam OR, Madacsi DP (1976) ESR investigation of the $[Al]^0$ centre in tetragonal GeO_2. Phys Rev (B) 13:1960–1966

Stapelbroek M, Gilliam OR, Bartram RH (1977) Transferred hyperfine interactions for trapped hole centers in tetragonal GeO_2. Phys Rev (B) 16:37–43

Stevens KWH (1952) Matrix elements and operator equivalents connected with the magnetic properties of rare-earth ions. Proc Phys Soc (A) 65:209–215

Strutt RJ (1914) Note on colour in zircons, and its radioactive origin. Proc Roy Soc (A) 89:405–407

Tennant WC (1976) Crystal-field operators in the Zeeman representation. Molec Phys 31:1505–1510

Tennant WC, Claridge RFC (1999) Large magnitude high-spin nuclear parameters in a Ti^{3+} centre from X-band EPR measurements at 10 K. J Magn Reson 137:122–131

Tennant WC, Walsby CJ, Claridge RFC, McGavin DG (2000) Rotation matrix elements and further decomposition functions of two-vector tesseral spherical tensor operators; their uses in electron paramagnetic resonance spectroscopy. J Phys Condens Matter 12:9481–9495

Thorpe AM, Briggs T, Tsang T, Senftle F, Alexander C (1977) Anisotropic magnetic susceptibility of erbium and ytterbium in zircon, $ZrSiO_4$. J Phys Chem Solids 38:477–480

Tuszynski JA, Buckmaster HA, Chatterjee R, Boteler JM (1985) Point-group discrimination using c-axis angular variation of the EPR fine-structure spectra for S-state ions. J Magn Reson 63:241–254

Uhrin R, Belt RF, Puttbach RC (1974) The hydrothermal growth of zircon. J Crystal Growth 21:65–68

Valishev RM, Vinokurov VM, Zaripov MM, Stepanov VG (1965) Electron paramagnetic resonance of Er^{3+} ions in crystals of zircon ($ZrSiO_4$). Geokhimiya 1:1265–1267

Vannotti LE, Morton JR (1968) Paramagnetic-resonance spectra of S^- trapped in alkali halide crystals. Phys Rev 174:488–453

Vaz JE, Senftle FE (1971) Thermoluminescence study of natural radiation damage in zircon. J Geophys Res 76:2038–2050

Vegard L (1926) Results of crystal analysis, part II, the zircon group. Phil Mag, Ser 7, 1:1158–1168

Vinokurov NM (ed) (1974) Magnetic and optical spectroscopy of minerals and rocks. Izd Kazan Univ: Kazan, USSR

Vinokurov VM, Gainullina NM, Evgrafova LA, Nizamutdinov NM, Suslina AN (1971) Zr^{4+}-Y^{3+} isomorphism and features of accompanying charge compensation in zircon crystals. Kristallografiya 16:318–323 (Sov Phys Crystall 16:262–265)

Vinokurov VM, Gainullina NM, Nizamutdinov NM, Krasnobaev AA (1972) Distribution of admixed Fe^{3+} ions in the single zircon crystals from the kimberlite pipe MIR. Geokhimiya 11:1402–1405

Vinokurov VM, Gainullina NM, Nizamutdinov NM (1974) EPR of iron (3+) and manganese (2+) ions and some radiation centres in zircon. In: Magnetic and optical spectroscopy of minerals and rocks. Kazan State University, Kazan, USSR

Vinokurov VM, Stepanov VG (1967) Magnitude of the initial splittings of gadolinium ions in crystals of the scheelite series. Sov Phys – Solid State 9:844–846

Vinokurov VM, Zaripov MM, Stepanov VG, Chirkin GK, Shekun LYa (1963a) Paramagnetic resonance of Nb^{4+} ions in zircon single crystals. Fiz Tverd Tela 5:2034–2035

Vinokurov VM, Zaripov MM, Pol'skii YuE, Stepanov VG, Chirkin GK, Shekun LYa (1963b) Detection by paramagnetic resonance of small amounts of Eu^{2+}, Gd^{3+}, Nb^{4+} and their isomorphism in fluorite and zircon. Geokhimiya 11:1002–1007

Walsby CJ (1999) Theoretical and experimental electron paramagnetic resonance studies of single crystals. PhD Thesis, Chemistry Department, University of Canterbury, New Zealand

Walsby CJ, Lees NS, Tennant WC, Claridge RFC (2000) 15-K EPR of an oxygen-hole boron centre, $[BO_4]^0$, in X-irradiated zircon. J Phys Condens Matter 12:1441–1450

Weil JA (1973) Use of symmetry-related crystal sites for measuring tensor properties in magnetic resonance. J Magn Reson 10:391–393

Weil JA (1984) A review of electron spin resonance spectrosopy and its application to the study of paramagnetic defects in crystalline quartz. Phys Chem Miner 10:149–165

Weil JA, Rao PS (2000) EPR/ENDOR frequency table (Bruker Almanac).

Weil JA, Buch T, Clapp JE (1973) Crystal point-group symmetry and microscopic tensor properties in magnetic resonance spectroscopy. Adv Magn Reson 6:183–257

Weil JA, Bolton JR, Wertz JE (1994) Electron paramagnetic resonance. Elementary theory and practical applications. Wiley, New York

White EW, Gibbs GV (1967) Structural and chemical effects on the SiK_β X-ray line for silicates. Am Mineral 52:985–993

Wykoff RWG, Hendricks SB (1928) Die Kristallstruktur von Zircon und die Kriterien für spezielle Lagen in tetragonalen Raumgruppen. Z Kristallogr 66:73–102

Xiaoyu H, Gui-Ru B, Min-Guang Z (1985) The study of the optical and the EPR spectra of V^{4+} in zircon-type crystals. J Phys Chem Solids 46:719–720